

THERMAL CHARACTERIZATION OF  
HOMOPOLYMERS, COPOLYMERS AND METAL FUNCTIONAL  
COPOLYMERS OF VINYL PYRIDINES

A THESIS SUBMITTED TO  
THE GRADUATE SCHOOL OF NATURAL AND APPLIED SCIENCES  
OF  
MIDDLE EAST TECHNICAL UNIVERSITY

BY

AYŞEGÜL ELMACI

IN PARTIAL FULFILLMENT OF THE REQUIREMENTS  
FOR  
THE DEGREE OF MASTER OF SCIENCE  
IN  
POLYMER SCIENCE AND TECHNOLOGY

SEPTEMBER 2008

Approval of the thesis:

**THERMAL CHARACTERIZATION OF HOMOPOLYMERS, COPOLYMERS  
AND METAL FUNCTIONAL COPOLYMERS OF VINYL PYRIDINES**

submitted by **AYŞEGÜL ELMACI** in partial fulfillment of the requirements for  
the degree of **Master of Science in Polymer Science and Technology**  
**Department, Middle East Technical University** by,

Prof. Dr. Canan Özgen \_\_\_\_\_  
Dean, **Graduate School of Natural and Applied Sciences**

Prof. Dr. Cevdet Kaynak \_\_\_\_\_  
Head of Department, **Polymer Science and Technology**

Prof. Dr. Jale Hacaloğlu \_\_\_\_\_  
Supervisor, **Chemistry Department, METU**

Prof. Dr. Ceyhan Kayran \_\_\_\_\_  
Co-Supervisor, **Chemistry Department, METU**

**Examining Comitee Members:**

Prof. Dr. Leyla Aras \_\_\_\_\_  
Chemistry Dept., METU

Prof. Dr. Jale Hacaloğlu \_\_\_\_\_  
Chemistry Dept., METU

Prof. Dr. Ceyhan Kayran \_\_\_\_\_  
Chemistry Dept., METU

Prof. Dr. Cevdet Kaynak \_\_\_\_\_  
Materials and Metallurgical Sciences Dept., METU

Assoc. Prof. Dr. Göknur Bayram \_\_\_\_\_  
Chemical Engineering, Dept., METU

Date: 02.September.2008

**I hereby declare that all information in this document has been obtained and presented in accordance with academic rules and ethical conduct. I also declare that, as required by these rules and conduct, I have fully cited and referenced all materials and results that are not original to this work.**

Name, Lastname: Ayşegül Elmacı

Signature:

# ABSTRACT

## THERMAL CHARACTERIZATION OF HOMOPOLYMERS, COPOLYMERS AND METAL FUNCTIONAL COPOLYMERS OF VINYL PYRIDINES

Elmacı, Ayşegül

Master of Science, Department of Polymer Science and Technology

Supervisor: Prof. Dr. Jale Hacaloğlu

Co-Supervisor: Prof. Dr. Ceyhan Kayran

September 2008, 65 pages

Although, the use of vinyl pyridine polymers, especially as matrices for nanoparticle synthesis, is growing considerably, the knowledge of thermal degradation behavior is still missing in the literature. In this study, thermal degradation characteristics of the homopolymers; poly(4-vinylpyridine), P4VP, and poly(2-vinylpyridine), P2VP, the diblock copolymers; polystyrene-block-poly(2-vinylpyridine), (PS-b-P2VP) and polystyrene-block-poly(4-vinylpyridine), (PS-b-P4VP), and the metal functional vinyl polymers; cobalt-polystyrene-block-poly(2-vinylpyridine) and cobalt-polystyrene-block-poly(4-vinylpyridine) were investigated by direct pyrolysis mass spectrometry. The effects of the position of the nitrogen in the pyridine ring, composition and molecular weight of diblock copolymer and coordination of the metal to the pyridine ring of the copolymer on thermal behavior were also investigated. The results showed that unlike most of the vinyl polymers that decompose via depolymerization, P2VP degrades through opposing reaction pathways; depolymerization, proton transfer to N atom in the pyridine ring yielding unsaturated linkages on the polymer backbone that decompose slightly at higher temperatures and loss of pyridine units. On the other hand the thermally less stable P4VP decomposition follows

depolymerization in accordance to general expectations. Another finding was the independent decomposition of both components of the diblock polymers, (PS-b-P2VP) and (PS-b-P4VP). Thermal degradation occurs in two main steps, the thermally less stable P2VP or P4VP chains degrade in the first step and in the second step decomposition of PS takes place.

It was also concluded that upon coordination of metal, thermal stability of both P2VP and P4VP increases significantly. For metal functional diblock copolymers thermal degradation of chains coordinated to Co metal through N in the pyridine ring occurred in three steps; cleavage of pyridine coordinated to Co, coupling and H-transfer reactions yielding unsaturated and/or crosslinked structure and decomposition of these thermally more stable unsaturated and/or crosslinked blocks. TEM imaging of the metal functional block copolymers along with the results of the pyrolysis mass spectrometry pointed out that PS-b-P2VP polymer is a better and more effective matrix for nanoparticle synthesis.

**Keywords:** Poly(2-vinylpyridine), poly(4-vinylpyridine), thermal degradation, polystyrene-block-poly(2-vinylpyridine), pyrolysis mass spectrometry,

# ÖZ

## POLİVİNİLİRİDİN HOMOPOLİMERLERİNİN, BLOK KOPOLİMERLERİNİN VE METAL FONKSİYONLU KOPOLİMERLERİNİN İSİSAL OLARAK KARAKTERİZASYONLARI

Elmacı, Ayşegül

Yüksek Lisans, Polimer Bilim ve Teknolojisi Bölümü

Tez Yöneticisi: Prof. Dr. Jale Hacaloğlu

Ortak Tez Yöneticisi: Prof. Dr. Ceyhan Kayran

Eylül 2008, 65 sayfa

Vinil piridin polimerlerinin özellikle nanoparçacık sentezinde kalıp olarak kullanımları gittikçe yaygınlaştığı halde, literatürde, bu polimerlerin ısısız bozunum davranışları hakkındaki bilgiler hala eksik bulunmaktadır. Bu çalışmada, poli(2-vinilpiridin), (P2VP) ve poli(4-vinilpiridin), (P4VP) homopolimerlerinin, polisitiren-blok-poly(2-vinilpiridin), (PS-b-P2VP), polisitiren-blok-poli(4-vinilpiridin), (PS-b-P4VP) diblok copolimerlerinin, ve metal fonksiyonlu kobalt-polisitiren-blok-poli(2-vinilpiridin) ile kobalt-polisitiren-blok-poli(4-vinilpiridin) vinil polimerlerinin ısısız bozunum karakteristikleri direkt piroliz kütle spektrometresi kullanılarak incelenmiştir. Piridin halkasındaki nitrogen atomunun konumunun, diblock kopolimerlerin kompozisyonlarının ve moleküler ağırlıklarının ve son olarakda kopolimerdeki piridin halkasına bağlanan metalin ısıl davranım üzerindeki etkileri de ayrıca incelenmiştir. Sonuçlar göstermiştir ki, depolimerize olarak bozulan bir çok vinil polimerinin aksine, P2VP depolimerize olmanın yanısıra diğerlerine ters düşen reaksiyonlarla da bozunmaktadır. Piridin halkasındaki N atomuna proton transferi olmakta ve bud a polimer ana zincirinde biraz daha yüksek sıcaklıklarda

bozulan doymamış ve çapraz bağların oluşmasına ve/veya piridin halkalarının kaybına sebep olmaktadır. Isıl olarak daha kararsız olan P4VP polimeri ise beklenildiği gibi depolimerize yöntemiyle bozunmaktadır. Bir başka bulgu da PS-b-P2VP ve PS-b-P4VP diblok kopolimerlerinin bileşenlerinin birbirlerinden bağımsız olarak bozunmalarıdır. Isıl bozunum iki adımda gerçekleşmektedir; birinci adımda ısıl olarak daha kararsız olan P2VP veya P4VP zincirlerinin parçalanmakta ve ikinci adımda da PS bozunması gerçekleşmektedir.

Ayrıca metal bağlanmasının hem P2VP hem de P4VP polimerlerinin ısıl kararlılığını dikkat çeker bir ölçüde arttırdığı sonucuna varılmıştır. Metal fonksiyonlu diblok kopolimerler de, piridin halkasındaki N atomu üzerinden Co metaline bağlı zincirlerin ısıl bozunum mekanizması üç adımda gerçekleşmektedir. Co metaline bağlı piridin kopması, doymamış ve/veya çapraz bağlı yapılara sebep olan H transferi reaksiyonları ve ısıl olarak daha kararlı olan bu yapıların bozunması. Metal fonksiyonlu blok kopolimerlerinin TEM görüntülerinden ve piroliz kütle spektrometresinden elde edilen sonuçlar göstermiştir ki PS-b-P2VP polimeri nanoparçacık sentezi için daha iyi ve daha verimli bir kalıptır.

**Anahtar Kelimeler:** Poli(2-vinilpiridin), poli(4-vinilpiridin), ısıl bozunum, polisitiren-blok-poli(2-vinilpiridin), piroliz kütle spektrometresi.

To My Beloved Husband

For encouraging me to go back to school and for believing in me

To My Precious Mom, Dad and Sister

For their endless support

To My Dear Friend Şeniz

For always being there for me

And To My Dear Son Ege

For his patience.

## ACKNOWLEDGEMENTS

This research was made easier with the guidance and extensive knowledge of my supervisor Prof. Dr. Jale Hacaloğlu. She has a very kind and lovely soul. I am very fortunate to have the chance of working with her.

I'd also like to thank my co-advisor Prof. Dr. Ceyhan Kayran for her support and her work with Kadir Kaleli in synthesizing the organometallic polymers.

I would like to give my thanks to Prof. Dr. Nikos Hadjichristidis (National and Kapodistrian University of Athens) for sending us the copolymers, thus providing us our first samples.

Many thanks to Assist. Prof. Dr. Tamer Uyar (iNANO - The University of Aarhus, Denmark), for taking the TEM images of our polymers.

I also appreciate Kadir Kaleli for his moral support. It was fun to work with him.

Many thanks to Yusuf Nur for answering my never ending questions.

I'd like to thank to Neslihan Gökçe , Zeynep Koyuncu, Arzu Yavuz and Gözde Tuzcu for their bighearted friendships through my master years.

I also want to thank to my mother and father in law for their support.

I am so grateful to my mother, father and sister for always having my back.

This thesis is part of a project that is partially supported by *TUBITAK Research Fund TBAG-106T656*.

# TABLE OF CONTENTS

ABSTRACT.....	iv
ÖZ.....	vi
ACKNOWLEDGEMENTS.....	ix
TABLE OF CONTENTS.....	x
LIST OF TABLES.....	xii
LIST OF SCHEMES.....	xiii
LIST OF FIGURES.....	xiv
CHAPTER	
1. INTRODUCTION.....	1
1.1 THERMAL DEGRADATION.....	2
1.2 PYROLYSIS.....	3
1.2.1 Py-GC/Mass Spectrometry.....	3
1.2.2 DP-Mass Spectrometry.....	4
1.3 MASS SPECTROMETRY.....	5
1.3.1 The Ion Source.....	6
1.3.2 The Analyzer.....	7
1.4 BLOCK COPOLYMERS.....	8
1.5 POLYSTYRENE-BLOCK-POLY(2-VINYLPYRIDINE).....	9
1.5.1 Polystyrene.....	10
1.5.2 Polyvinylpyridines.....	12
1.6 METAL CARBONYL COMPLEXES.....	13
1.6.1 Dicobalt Octacarbonyl.....	13
1.7 AIM OF THE WORK.....	14
2. EXPERIMENTAL.....	15

2.1	MATERIALS .....	15
2.1.1	Homopolymers .....	15
2.1.2	Chemicals .....	16
2.2	SYNTHESIS AND CHARACTERIZATION OF METAL FUNCTIONAL DIBLOCK COPOLYMERS.....	17
2.2.1	Fourier Transform Infrared (FTIR).....	17
2.2.2	Transmission electron Microscope (TEM).....	18
2.2.3	Direct Pyrolysis Mass Spectrometry (DP-MS).....	18
2.2.4	Thermal Gravimetric Analysis (TGA) .....	19
3.	RESULTS AND DISCUSSION .....	20
3.1	PYROLYSIS OF HOMOPOLYMERS.....	20
3.1.1	Polystyrene .....	20
3.1.2	Poly(2-vinylpyridine).....	22
3.1.3	Poly (4-vinylpyridine).....	30
3.2	PYROLYSIS OF DIBLOCK COPOLYMERS .....	34
3.2.1	PS-b-P2VP Diblock Copolymer .....	34
3.2.2	PS-b-P4VP Diblock Copolymer .....	42
3.3.	METAL FUNCTIONAL POLYMERS.....	46
3.2.3	Cobalt-PS-b-P2VP Diblock Copolymer .....	47
3.2.4	Cobalt-PS-b-P4VP Diblock Copolymer .....	54
4.	CONCLUSION .....	60
	REFERENCES .....	62

## LIST OF TABLES

Table 2-1: Molecular weights of PS homopolymers.....	15
Table 2-2: Characteristics of the polymers obtained from Polymer Source Inc. ....	16
Table 2-3: Characteristics of PS-b-P2VP polymers with different compositions ..	16
Table 3-1: The relative intensities (RI) and assignments made for the intense and/or characteristic peaks present in the pyrolysis mass spectrum (Py-MS) of PS50400 at 445 °C.....	22
Table 3-2: RI and assignments made for the intense and/or characteristic peaks present in the (Py-MS) of P2VP-1 Mw: 11000 at 435 °C and P2VP-2 Mw: 64000 at 436 °C.....	25
Table 3-3: Peak assignments of P4VP polymer.....	33
Table 3-4: Peak assignments of PS-b-P2VP diblock copolymer.....	39
Table 3-5: Peak assignments for PS-b-P4VP polymer.....	44
Table 3-6: Peak assignments for Co-PS-b-P2VP.....	51
Table 3-7: Peak assignments for Co-PS-b-P4VP.....	57

## LIST OF SCHEMES

Scheme 1-1: Depolymerization by main chain cleavage and styrene monomer formation. ....	11
Scheme 1-2: a) Monomer and benzyl radical formations or b) Trimer formation. ....	11
Scheme 1-3: Dimer Formation.....	12
Scheme 3-1: Hydrogen transfer a) Inter chain b) Intra chain to the N atom. ....	27
Scheme 3-2: Possible mechanism for the loss of pyridine .....	30
Scheme 3-3: Possible results of the interaction of metal with the pyridine ring .....	50

## LIST OF FIGURES

Figure 1-1: Parts of a mass spectrometer .....	6
Figure 1-2: a) Replacement of C-H with Nitrogen forms a different type of polymer <sup>[14]</sup> .....	9
Figure 1-3: a) 2-vinylpyridine monomer and b) 4-vinylpyridine monomer .....	12
Figure 2-1: FTIR spectra of PS-b-P2VP vs. Co-PS-b-P2VP polymers <sup>[41]</sup> .....	18
Figure 3-1: a) The total ion current (TIC) curve detected during the pyrolysis of PS samples and b) Mass spectrum at 445 °C for PS50400. ....	21
Figure 3-2: TGA curves of a) P2VP-1 and b) P2VP-2 .....	23
Figure 3-3: a) The TIC curve and b) Mass spectrum at 435 °C of P2VP-1 .....	24
Figure 3-4: Pyrograms showing the H transfer and loss of Py ring in P2VP-1 .....	26
Figure 3-5: a) The TIC curve for P2VP and b) Mass spectrum at 436 °C of P2VP-2 .....	28
Figure 3-6: Comparison of single ion pyrograms for a) P2VP-2 and b) P2VP-1 polymers.....	29
Figure 3-7: TGA curve for P4VP .....	31
Figure 3-8: a) TIC curve and b) Spectrum of P4VP homopolymer at 438 °C.....	31
Figure 3-9: P4VP pyrograms showing the lack of hydrogen transfer to N atom..	34
Figure 3-10: TGA results for the PS-b-P2VP.....	35
Figure 3-11: The effect of composition change in the PS-b-P2VP diblock copolymers.....	36
Figure 3-12: a) The TIC Curve and b) Pyrolysis mass spectra recorded for PS-b- P2VP-1. ....	37
Figure 3-13: Single ion pyrograms of some selected products of PS-b-P2VP-1 .....	40
Figure 3-14: Comparison of a) PS-b-P2VP-1 and b) PS-b-P2VP-2 copolymers. ....	41
Figure 3-15: TGA for PS-b-P4VP copolymer .....	42

Figure 3-16: a) The TIC curve and b) Spectrum at two maxima for PS-b-P4VP polymer.....	43
Figure 3-17: Single ion pyrograms of some selected products of PS-b-P4VP.....	45
Figure 3-18: TIC curve and spectrum for a) Refluxed PS-b-P2VP and b) PS-b-P2VP .....	46
Figure 3-19: TEM image for Co-PS-b-P2VP polymer.....	47
Figure 3-20: TGA of the Co-PS-b-P2VP organometallic polymer .....	48
Figure 3-21: a) The TIC curve and b) Spectrum at the peak maximum and at the shoulder.....	49
Figure 3-22: Comparison of the metal functional polymer with PS-b-P2VP a) TIC curves and b) Pyrolysis mass spectra.....	50
Figure 3-23: SIP of some selected characteristic products of Co-PS-b-P2VP polymer.....	52
Figure 3-24: TEM images of Co-PS-b-P4VP.....	54
Figure 3-25: a) The TIC curve and b) Spectrum at the two peak maxima for Co-PS-b-P4VP .....	55
Figure 3-26: Comparison of the metal functional polymer with PS-b-P4VP a) TIC curves.....	56
Figure 3-27: Single ion evolution profiles of some selected characteristic products of Co-PS-b-P4VP polymer.....	58

# CHAPTER 1

## INTRODUCTION

An organometallic polymer is any macromolecule that contains both organic and metallic (i.e., transition-metal containing) moieties <sup>[1]</sup>. Organometallic polymers offer the ability to prepare functional macromolecules that combine the physical and electronic properties of organic polymers with the physical, electronic, optical, and catalytic properties inherent to organometallic complexes <sup>[1]</sup>. The transition metal centers in the polymers have the ability to change oxidation states and/or facilitate electron flow in ways that organic materials simply cannot. There are two classes of organometallic polymers, depending on the position of the metal atom relative to the primary polymer backbone; side group (SGOPs) and main chain organometallic polymers. SGOPs have an “all-organic” polymer backbone, which means that the polymeric structure is present regardless of the presence of the metal atoms <sup>[1]</sup>.

The synthesis of organometallic polymers by coordination of metals to plastics or other polymeric materials has gained significant interest as a consequence of their uses as conductors, liquid crystals, light emitting diodes and their interesting optical, magnetic and catalytic characteristics. On the other hand the use of organometallic polymers for the preparation of nano structural metallic composites increases the importance of these materials even more. The literature work indicates that the use of block copolymers, with interesting morphologic characteristics, in the synthesis of organometallic polymers yields several advantages in the preparation of nano structural metal composites <sup>[2]</sup>. Though

several studies on preparation and application of these important materials have been carried out, the knowledge of reaction mechanism and thermal characteristics that are very important for investigation of synthesis routes and application areas is still limited. Furthermore, it is also known from the previous studies that the temperature control has significant importance in the preparation of nano structural metallic composites. The reaction temperature should be high enough to decompose precursor, yet, it should be sufficiently low to avoid degradation of the polymeric structure. The decomposition of the polymer leads aggregation of the nano particles. Thus, the knowledge of the effect of temperature on organometallic polymer precursor has significant importance.

## 1.1 THERMAL DEGRADATION

There are various techniques to analyze the thermal behavior of polymers, such as *Thermal Gravimetric Analysis* (TGA) in which the change in the mass of a sample is measured as a function of temperature or time. The variation of mass in the sample may be because of the volatile products generated as a result of chemical reactions during heating of the sample <sup>[3]</sup>. These reactions can be combustion, dehydration, decomposition, etc. Another technique is *Differential Scanning Calorimetry* by which the glass transition temperature or the percent crystallinity of a polymer can be determined by simply heating the polymer sample with respect to a reference and calculating the enthalpy differences. An alternative technique for analyzing the polymer degradation mechanisms is called *Pyrolysis*; this technique may be coupled to a mass spectrometer and it is explained in detail below.

## 1.2 PYROLYSIS

Pyrolysis is thermal degradation of materials in an inert atmosphere or vacuum. Thermal stability depends on the relative strengths of the bonds which hold the molecule together. As a result of heating, the thermal energy may be distributed about all modes of excitation and when vibrational excitation is greater than the energy of specific bonds, the molecule will fragment. Pyrolysis temperature has significant importance on product distribution along with the heating rate. Pyrolysis is widely applied to investigate thermal characteristics of a compound such as, thermal stability, degradation products and decomposition mechanism. It is also used as a pre-processing step to convert large molecules into lower mass molecules that are easily detectable. For instance, when polymers are pyrolyzed, smaller fragments, oligomers, are produced and analysis of these fragments aids in the identification of the polymers.

Pyrolysis technique can be coupled with FT-IR, GC (Py-GC), GC/MS (Py-GC/MS) or MS (DP-MS). Among these various analytical pyrolysis techniques, pyrolysis gas chromatography mass spectrometry, Py-GC/MS or direct pyrolysis mass spectrometry, DP-MS, have several advantages such as sensitivity, reproducibility, minimal sample preparation and consumption and speed of analysis<sup>[4]</sup>.

### 1.2.1 Py-GC/Mass Spectrometry

In case of Pyrolysis gas chromatography mass spectrometry technique (Py-GC/MS), pyrolysis takes place near the GC injection port where complex thermal degradation products are separated by the gas chromatograph prior to analysis by the mass spectrometer. Analysis takes place in three steps; *thermal degradation*

of the sample, *separation* of the thermal degradation products by the GC column, *detection* of all the separated components by MS.

Each individual peak components of the specific pyrogram can be identified based on their mass spectra. Thus, identification of the pyrolyzates is rather simple. However, secondary reactions cannot be eliminated and there is always the possibility of not detecting some of the thermal degradation products that retained in the pyrolytical zone, injection system or capillary column as a consequence of molecular weight and high polarity. Furthermore, only stable thermal degradation products can be detected with the use of this technique.

### **1.2.2 DP-Mass Spectrometry**

In this method, pyrolysis is conducted inside the mass spectrometer, close to the ion source, using the direct inlet probe to benefit from the high vacuum and the immediate analysis after pyrolysis <sup>[5]</sup>. The analysis takes place in four steps; *thermal degradation* of the sample, *ionization* of thermal degradation products, *fragmentation* of ionized species involving excess energy and *detection* of all ions generated by MS.

The high vacuum inside the mass spectrometer favors vaporization and thus allows the analysis of higher molecular mass pyrolyzates. As the high vacuum system rapidly removes the degradation products from the heating zone, secondary reactions and condensation reactions are avoided. Furthermore, because of the rapid detection system of the mass spectrometers, unstable thermal degradation products can also be detected. Scanning total ion current (TIC) pyrogram as a function of temperature allows separation of components present in the sample as a function of volatility and/or thermal stability.

However, as the mixture of various thermal degradation products further dissociates during the ionization the mass spectra are usually very complex.

DP-MS is a very useful tool used to identify the polymers and their degradation products. The advantages of this technique are; the rapid detection of the pyrolysis products, the detection of high molecular weight products and the determination of primary degradation products. These pyrolysis products are indicative of the polymer degradation pathways and the polymer structure [6]. However, the main drawback of the method lies in the interpretation of the immense data obtained [7].

Today, DP-MS is a preferred method in many fields, as the technique eliminates the isolation and amplification steps necessary to separate the components under investigation from a complex chemical, clinical or environmental matrix and provides fast identification on the basis of the analytical fingerprint formed by the degradation products.

### **1.3 MASS SPECTROMETRY**

Mass Spectrometry is a powerful and a sensitive technique for identifying unknowns and studying molecular structure. Since its discovery in 1950s it is used in some important applications such as; trace element analysis, molecular weight determinations, quantitative and qualitative analysis of all type of substances even polymers, analysis of proteins, peptides, single cells in biotechnology, water quality, food contamination in environmental science and even used in space, in the exploration of Mars [8], [9].

The basic principle of mass spectrometry (MS) is to generate ions from a sample by any suitable ionization method, to separate these ions by their mass to charge ratio ( $m/z$ ) and to detect them quantitatively and qualitatively by their respective  $m/z$  abundance <sup>[10]</sup>. A mass spectrometer consists of three main sections; an ion source, a mass analyzer and a detector, all of which operates under high vacuum (Figure 1-1). Output from the detector is sent to a computer and the results are displayed in the form of a **mass spectrum** which is a graph of ion intensity as a function of mass to charge ratio <sup>[11]</sup>. Selective ion monitoring is also possible. A mass spectrometer can be coupled to various chromatography techniques such as GC, HPLC etc or to a pyrolyzer. For these analyses, variation of total ion current, TIC, as a function of time or temperature can be obtained.

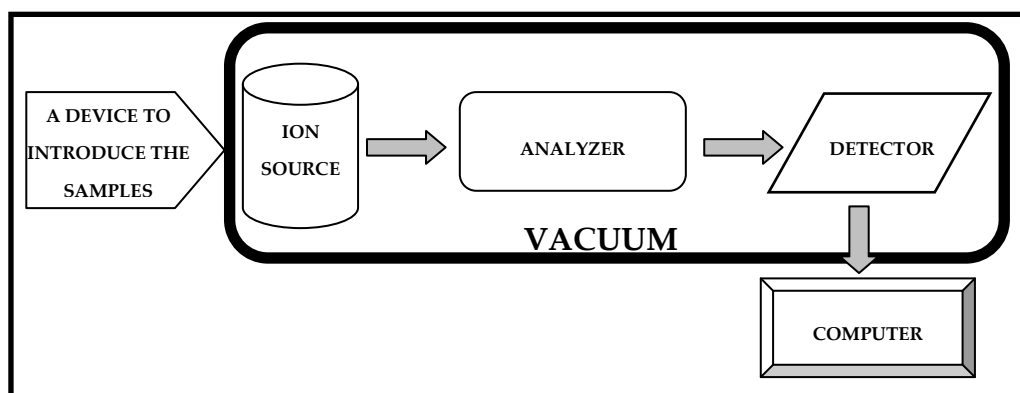


**Figure 1-1:** Parts of a mass spectrometer

### 1.3.1 The Ion Source

Sample to be analyzed must first be ionized because the mass analyzer can only deal with charged species. This takes place in the ion source. For a mass spectral analysis, formation of gaseous ions is necessary. Depending on the ionization method used, the sample is converted to molecular or quasi molecular ions and their fragments <sup>[12]</sup>. Various types of ion sources such as Electron Impact (EI),

Chemical Ionization (CI), Photo Ionization (PI), Matrix Assisted Laser Desorption Ionization (MALDI), Electrospray Ionization (ES) and Fast Atom Bombardment (FAB) etc are available. The choice depends on the purpose of the user and the type of chemicals to be worked on, along with the price of the ion source and the amount of the samples. EI sources are the most commonly used ones and most of the library data were obtained using *Electron Impact Ion Source*.

#### **1.3.1.A *Electron Impact Ion source (EI)***

The molecules in the gas phase are bombarded with electrons that have sufficient energy to ionize the molecules. At around 10 eV most of the organic molecules can be ionized. As the electron energy is increased, the fragmentation of the molecule and the total ion yield also increase. At 70 eV the total ion yield reaches a plateau. Therefore, for reproducibility of the data obtained, working at this energy level is important. After the molecules are bombarded with the electrons, they become charged species and pushed into the mass analyzer by an ion repeller, where they will be separated according to their mass to charge ratios ( $m/z$ ).

For polymers, upon heating, the volatile species are produced. These decomposition products are bombarded with electrons to produce charged species.

#### **1.3.2 The Analyzer**

The charged particles reaching the mass analyzer are separated according to their mass to charge ratios;  $m/z$ . There are several types of analyzers such as magnetic, time of flight and quadrupole, quadrupole ion trap...etc.

### 1.3.2.A *Quadrupole Analyzer*

Quadrupole analyzers are rapid scanning devices. They are preferred because of their high transmission, light weight, compactness and low price, lower ion acceleration voltage and higher scan speeds <sup>[10]</sup>.

## 1.4 **BLOCK COPOLYMERS**

During the last decades, the studies on the incorporation of nanomaterials with block polymers have been the subject of many researches. The dominant reason to be, in block copolymers, the interactions between the different blocks form micro domains, where similar blocks group together near each other forming meso phases. The covalent bonds linking the unlike blocks are localized in the surrounding area of the microdomain interfaces <sup>[13]</sup>, <sup>[14]</sup>. Because of this covalent bonding between the segments, the system can not macroscopically phase separate, and so it minimizes the interfacial energy by adopting well-defined microdomain patterns <sup>[15]</sup>. These patterns formed are the basis for many studies in organometallic and/or metal functional polymers <sup>[16]</sup>.

Block copolymers also have the desirable feature that their morphology can be systematically controlled by varying the number of blocks, their lengths, and their chemical compositions. For example, diblock copolymers can form cubic arrays of spheres, hexagonal arrays of cylinders, bi continuous cubic phases, or lamellae, depending on the relative block lengths <sup>[17]</sup>.

There are various preparation methods for block copolymers that can be found in detail in literature <sup>[18]</sup>, <sup>[19]</sup>, <sup>[20]</sup>. In this study, the diblock copolymer, polystyrene-

block-poly(2-vinylpyridine), (PS-b-P2VP), is for the preparation of metal functional polymer.

## 1.5 POLYSTYRENE-BLOCK-POLY(2-VINYLPYRIDINE)

One of the suitable block copolymers to make an organometallic complex or metal function polymer is found to be PS-b-P2VP diblock polymer. PS-b-P2VP, composed of a polar group P2VP and a hydrophobic group, PS, contains polar nano regions of a controllable size and shape that serve as excellent sites for the encapsulation of inorganic particles [21]. When metals are incorporated into these kind of polymer matrices, hybrid materials are formed.

Polystyrene-b-poly(2-vinylpyridine) copolymer can go under micro phase separation. The structures that form depend on the relative number of monomers in each block, for instance, when the number of monomers in each block is about the same, a lamellar structure forms as shown in Figure 1-2.

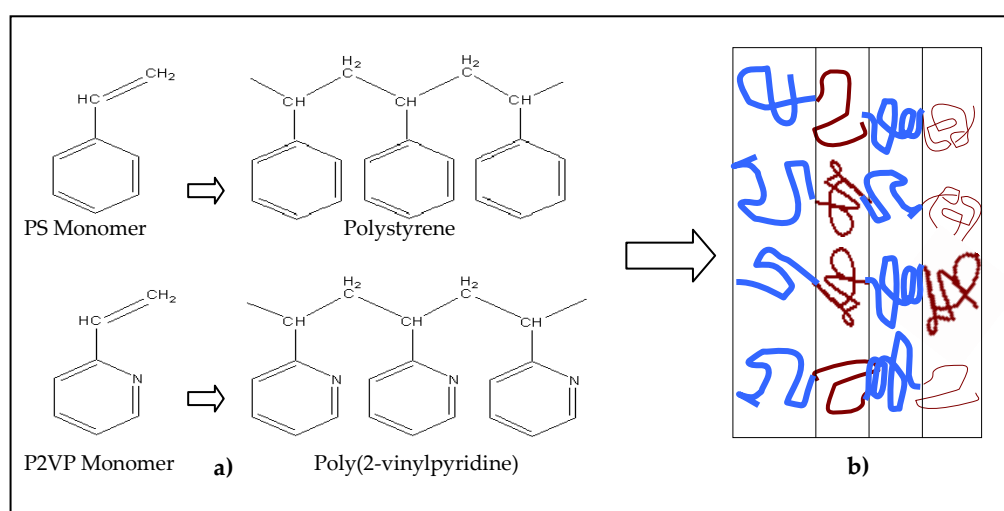


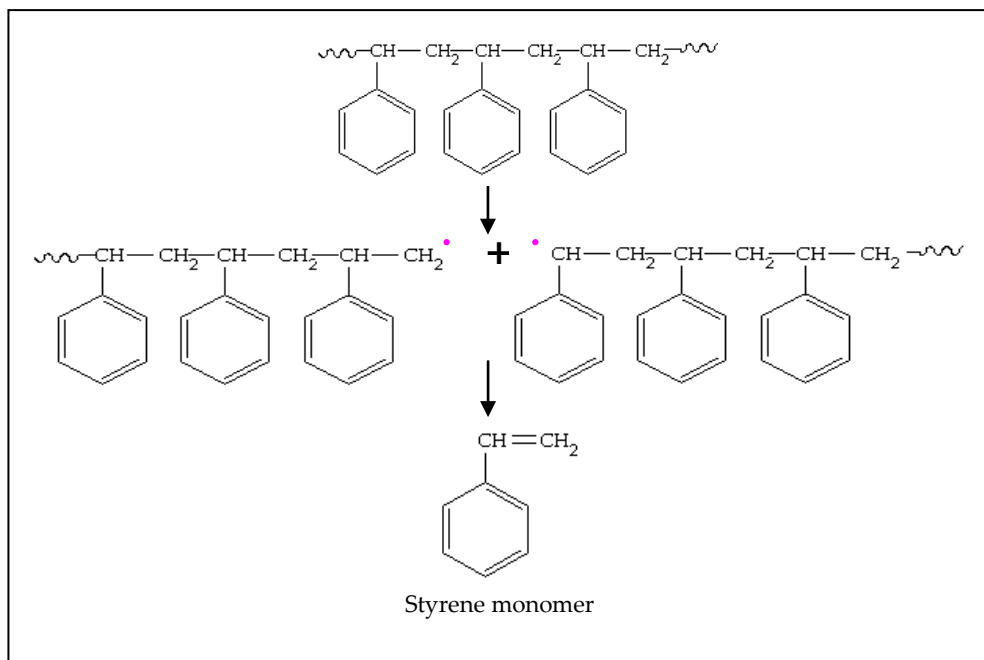
**Figure 1-2:** a) Replacement of C-H with Nitrogen forms a different type of polymer [14]  
b) Alike polymers gather together, forming mesophases.

PS-b-P2VP copolymer is extensively studied and used in nanoparticle assembling into block copolymers. Relevant work can be found in the literature on phase behavior, micelle formation and nanomaterial incorporation of PS-b-P2VP polymer [22]-[26]. In the PS-b-P2VP copolymer, the metal binding site is the nitrogen atom on the pyridine ring, because of the free electron pair on the nitrogen atom.

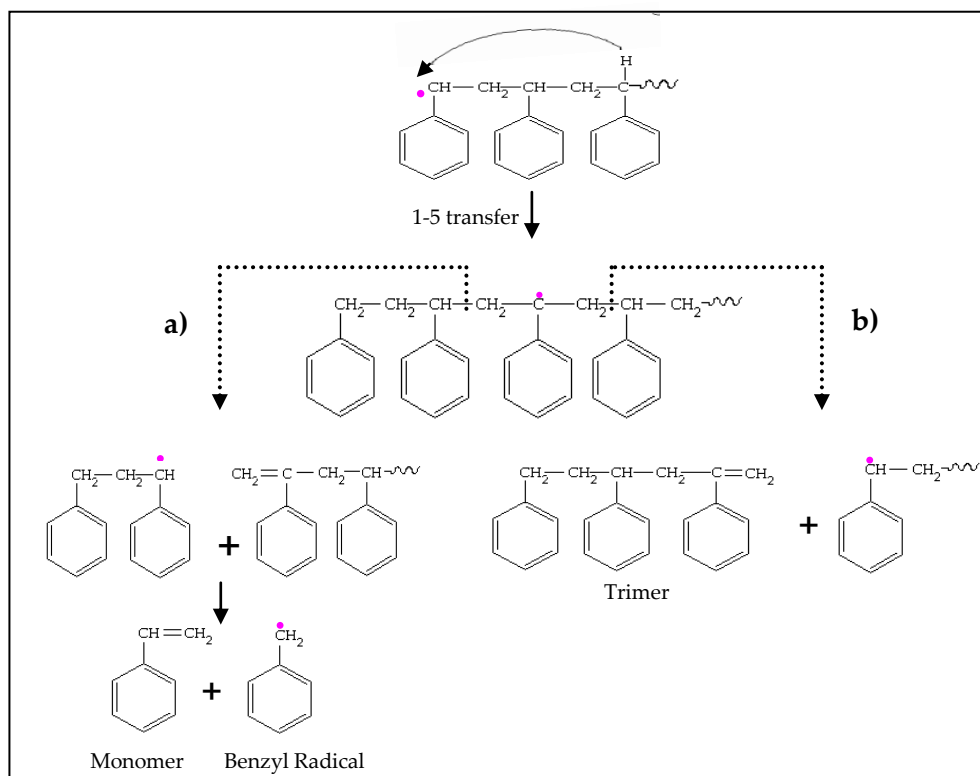
In order to understand the thermal behavior of diblock copolymers, the homopolymers composing it should be understood as well.

### 1.5.1 Polystyrene

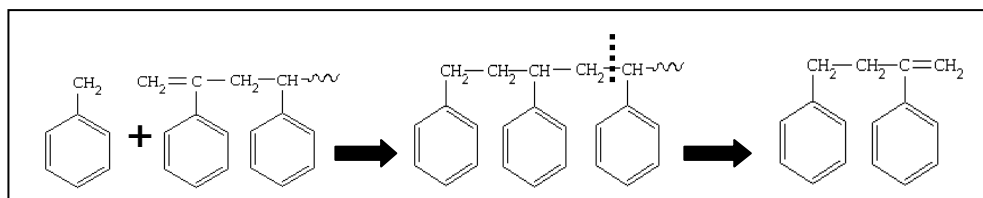
Polystyrene is an amorphous thermoplastic polymer. It is commonly used as research material for advanced materials. Polystyrene has widely been studied and therefore its thermal degradation mechanism is well understood [27]-[32]. It is known that PS degrades via radicallic depolymerization, yielding mainly monomer (Scheme 1-1), 1-5 Hydrogen transfer, also known as back biting reactions (Scheme 1-2), chain end scission yielding dimer and trimer also take place [33]. Thus, thermal degradation process generates mainly monomer and low molecular weight oligomers (Scheme 1-3).



**Scheme 1-1:** Depolymerization by main chain cleavage and styrene monomer formation.



**Scheme 1-2:** a) Monomer and benzyl radical formations or b) Trimer formation.



**Scheme 1-3:** Dimer Formation

### 1.5.2 Polyvinylpyridines

Vinylpyridine polymers have some interesting properties due to the presence of the nitrogen atom in the pyridine ring. The weakly basic nitrogen atom makes possible a variety of reactions on vinylpyridines <sup>[34]</sup>. The nitrogen atom has the capacity to coordinate with the metals <sup>[35]</sup>, so the polyvinylpyridines (PVP) act as a matrix for the metal nanoparticles. PVP polymers are easily available, soluble in slightly acidic aqueous media and in polar organic solvents, resistant to degradation by acids, alkalis, reductors and oxidants and they are thermally stable <sup>[21]</sup>.

Polyvinylpyridines have a great potential in the applications as polyelectrolytes, polymeric reagents and in electrical applications. They are also used as ion-exchange and macroporous resins <sup>[34]</sup>, <sup>[36]</sup>, The two most common PVP polymers are poly(2-vinylpyridine), (P2VP) and poly(4-vinylpyridine), (P4VP) (Figure 1-3).

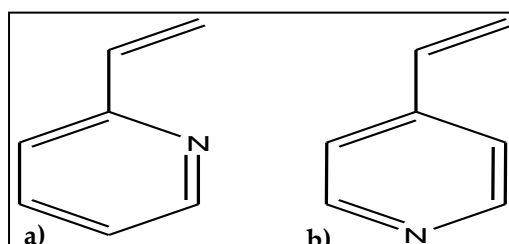


**Figure 1-3:** a) 2-vinylpyridine monomer and b) 4-vinylpyridine monomer

Kuo et al. <sup>[37]</sup> studied the two pyridine polymers and found out that P4VP has a greater ability to form hydrogen bonding with phenolics than P2VP. The reason for this was thought to be the steric hindrance effect on nitrogen atoms in P2VP.

Also, another study made by Zha et al.<sup>[38]</sup> showed that the order-disorder transition temperature ( $T_{ODT}$ ) of PS-b-P4VP diblock copolymer is remarkably high compared to that of PS-b-P2VP diblock copolymer. The reason for the much higher  $T_{ODT}$  of PS-b-P4VP diblock copolymers as compared with the  $T_{ODT}$  of PS-b-P2VP diblock copolymers is attributable to the stronger polarizability of P4VP in PS-b-P4VP diblock copolymer compared with the polarizability of P2VP in PS-b-P2VP diblock copolymer.

The degradation mechanism of the poly(2-vinylpyridine) polymers may be thought to be similar to that of the polystyrene because of the structural similarity. Yet, up to now, no study on thermal degradation mechanism of poly(2-vinylpyridine) has appeared in the literature.

## 1.6 METAL CARBONYL COMPLEXES

### 1.6.1 Dicobalt Octacarbonyl

Metals like *iron*, *cobalt*, *nickel* and a number of *alloys* possess a greater level of magnetism, which is called *ferromagnetism*, than other substances. This phenomenon is due to a large magnetic moment of the atoms of these metals, due to the unbalanced spin of the electrons in their inner orbits. Ferromagnetic materials are the topic of many researches in nanotechnology. Complexes of nickel, cobalt and iron are the most studied ones. Among them, cobalt is the one having the largest magnetic responsivity <sup>[39]</sup>. Cobalt-based magnetic materials are used in electronics, in high density storage media applications, catalysis and

biomedical sciences. Cobalt nanoparticles can be obtained via solution-phase metal salt reduction processes or decomposition of neutral organometallic precursors such as dicobalt octacarbonyl ( $\text{Co}_2\text{CO}_8$ )<sup>[40]</sup>.

There are various other transition metal carbonyl complexes used in the synthesis of organometallic polymers. Cobalt is the preferred one in this research because, the carbonyl disassociation occurs at lower temperatures than others, allowing the combination of the metal to the polymer at low temperature reaction medium. One drawback of carbonyl complex is that it is very sensitive to oxygen. Therefore, the experiments should be made under inert atmosphere.

## 1.7 AIM OF THE WORK

In this work, thermal degradation characteristics such as thermal stability, thermal degradation products and thermal degradation mechanism of the homopolymers; poly(4-vinylpyridine), poly(2-vinylpyridine) and polystyrene, the copolymers; polystyrene-block-poly(2-vinylpyridine) and polystyrene-block-poly(4-vinylpyridine) and the metal functional polymers; cobalt-polystyrene-block-poly(2-vinylpyridine) and cobalt-polystyrene-block-poly(4-vinylpyridine) were investigated. The effect of the position of the nitrogen in the pyridine ring on thermal behavior and bonding of the metal to the copolymers were also investigated.

## CHAPTER 2

### EXPERIMENTAL

#### 2.1 MATERIALS

##### 2.1.1 Homopolymers

**Polystyrene:** Polystyrene homopolymers were obtained from Middle East Technical University's Chemistry Department. Their characteristics are shown in Table 2-1.

**Table 2-1:** Molecular weights of PS homopolymers

Sample Name	Mw
PS50	50000
PS110	110000
PS280	280000
PS411	411000

**Polyvinylpyridines:** Homopolymers P2VP-1 and P2VP-2 (MW: 11000 and MW: 64000) and P4VP (MW: 60000) were purchased from Sigma Aldrich and used without further purification.

**Diblock Copolymers:** PS-b-P2VP and PS-b-P4VP polymers were purchased from Polymer Source Inc. and several PS-b-P2VP polymer samples with varying compositions were synthesized and characterized by Hadjiichristidis et. al. according to the literature methods [40]. In Table 2-2 and Table 2-3 characteristics of the commercially purchased and copolymers synthesized are given respectively.

**Table 2-2:** Characteristics of the polymers obtained from Polymer Source Inc.

Name	Polymer Source ID	Mn (PS)	Mn (PV)	HI (Mw/Mn)
PS-b-P2VP-1	P8722-S2VP	58000	16500	1.08
PS-b-P2VP-2	P3673-S2VP	25000	15000	1.04
PS-b-P4VP	P4966-S4VP	57500	18500	1.15

**Table 2-3:** Characteristics of PS-b-P2VP polymers with different compositions

Sample	MW (PS)	MW (Diblock)	I=Mw/Mn (Diblock)	%wt PS	%wt P2VP
S3	45000	50000	1.06	90	10
S4	40000	50000	1.09	80	20
S5	10000	18000	1.08	56	44
S6	4500	10000	1.16	44	56
S7	14000	33000	1.19	42	58

### 2.1.2 Chemicals

The transition metal complex, dicobalt octacarbonyl (ID number: 291840050), with a molecular weight of 341.95 gr. was acquired from Acros Organics and

used without further purification. The solvent toluene was purchased from Aldrich and was purified by refluxing over metallic sodium under nitrogen for two days.

## 2.2 SYNTHESIS AND CHARACTERIZATION OF METAL FUNCTIONAL DIBLOCK COPOLYMERS

The procedure followed to synthesize the metal functional block copolymers of vinylpyridines was explained in detail in the literature <sup>[41]</sup>. Shortly, all reactions were performed in a glow box under deoxygenated nitrogen atmosphere, since  $\text{Co}_2(\text{CO})_8$  is very sensitive to oxygen and quickly decomposes. 150 mg of block copolymer, PS-b-P2VP-1 or 2 or PS-b-P4VP was dissolved completely in 15 ml toluene (With a boiling point of 109 °C) and stirred for one hour. Then, 300mg of  $\text{Co}_2\text{CO}_8$  was added to this solution. The mixture was refluxed for eight hours at 110 °C, under deoxygenated nitrogen atmosphere. Toluene was then evaporated under vacuum and the resultant product was analyzed by means of TEM, FTIR TGA and direct pyrolysis mass spectrometry techniques.

### 2.2.1 Fourier Transform Infrared (FTIR)

FTIR analyses of the samples were performed by dropping a drop of sample on KBR pellet using *Nicolet 510 FTIR Spectrometer*. Theoretically, the nanoparticle formation starts by the coordination of the electron-rich segment of the copolymer, which is 2-vinylpyridine, or 4-vinylpyridine to the metal atom with the exclusion of the ligands. As a result of this bonding of pyridine nitrogen to the metal atom or ion, the pyridine stretching and bending modes should be affected <sup>[41]</sup>. In fact, the IR spectrum of the Co-PS-b-P2VP showed a decrease in the

intensities of the peaks related to pyridine and a new peak formation was observed at  $467\text{ cm}^{-1}$ , indicating the coordination of Co to N atom. A comparison of FTIRs of polymers PS-b-P2VP and Co-PS-b-P2VP gave evidence of cobalt bonding to the pyridine as stated (Figure 2-1).

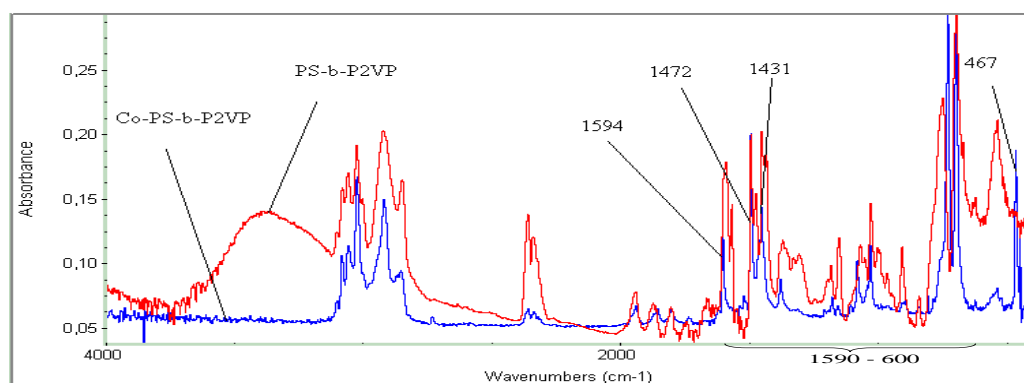


**Figure 2-1:** FTIR spectra of PS-b-P2VP vs. Co-PS-b-P2VP polymers <sup>[41]</sup>.

### **2.2.2 Transmission electron Microscope (TEM)**

TEM imaging of the nano particles was carried out with a *Philips CM20 instrument at a 200kV* (iNANO - The University of Aarhus, Denmark). The nano particles were dispersed on the carbon-coated copper grid from their diluted suspension of toluene.

### **2.2.3 Direct Pyrolysis Mass Spectrometry (DP-MS)**

DP-MS analyses were made by using *Waters Micromass Quattro Micro GC Mass Spectrometer* with a mass range is 10 to 1500 Da and EI ion source *coupled to a Direct Insertion Probe*. During the pyrolysis the temperature was increased to 50 °C at a rate of 5 °C/ min., then was raised to 650 °C with a rate of 10 °C/min. and

kept at 650 °C for 5 additional minutes while recording 70eV EI mass spectra at a mass scan rate of 1 scan/s.

Deep capillary quartz tubes were used as sample containers and the total ion curves (TIC) and single ion pyrograms (SIP) and pyrolysis mass spectra of the samples were analyzed by a special program called *MassLynx V4.1* copyrighted by Waters Cooperation.

#### **2.2.3.A Method of analysis**

For the analyses of pyrolysis mass spectra, the mass spectrum recorded at the TIC maximum is selected first. The next step is the identification of all intense peaks. The trends in the evolution profiles are used to group the products to determine whether the fragment is generated during pyrolysis or EI ionization.

For each peak in a given group, assignments are made and tabulated considering the mass differences and possible dissociation processes, classical fragmentation pathways for organic compounds and taking into consideration the structure of the sample under investigation.

#### **2.2.4 Thermal Gravimetric Analysis (TGA)**

TGA technique was used in order to understand the degradation kinetics of the copolymers and the synthesized organometallic polymers by using a *Perkin Elmer Pyris 1 TGA*, (Central Laboratory, METU) under nitrogen atmosphere. The temperature range worked was 25 °C to 700 °C and heating rate of the samples was 10 °C/min.

## CHAPTER 3

### RESULTS AND DISCUSSION

Thermal characterizations of PVPs, PVP-PS diblock copolymers and Co functional PVP-PS diblock copolymers were investigated by direct pyrolysis mass spectrometry technique. Pyrolysis mass spectrometry analyses of polystyrene were also performed. Furthermore, the effect of molecular weight on thermal characteristics, and composition of copolymer were also studied for PS, P2VP and PS-b-P2VP block copolymer. In order to get a better understanding, thermal degradation behaviors of diblock copolymers refluxed in toluene under the same conditions used in the synthesis of metal functional diblock copolymers, but in the absence of cobalt complex were also investigated. For some samples, thermal behaviors were also studied by TGA, yet, in general the  $T_{\max}$  values were lower and almost constant for only the samples under investigation.

#### 3.1 PYROLYSIS OF HOMOPOLYMERS

##### 3.1.1 Polystyrene

Thermal degradation of PS has been studied in detail in the literature <sup>[27]-[32]</sup>. It is known that PS degrades via radicalic depolymerization yielding mainly styrene monomer. 1, 5 - H transfer reactions also takes place yielding dimer and trimer.

The total ion current (TIC) curve that is the variation of total ion yield as a function of temperature, detected during the pyrolysis of PS samples with

variable molecular weights are shown in Figure 3-1. The pyrolysis mass spectral data indicated only a slight increase in thermal stability (a 9 °C shift to the high temperatures) as the molecular weight of the PS samples increased. Therefore, it can be concluded that the molecular weight in the range studied does not have a significant effect on the thermal stability of the PS samples.

The relative intensities of the characteristic and/or intense peaks present in the pyrolysis mass spectrum recorded at the peak maximum of the TIC curve of PS and the assignments made are summarized in Table 3-1. Monomer, dimer and trimer peaks at  $m/z = 104$ , 208 and 312 Da respectively, can easily be identified in accordance with the literature results. Most of the other peaks present in the pyrolysis mass spectra are due to the fragments generated during EI ionization of these products; i.e. peaks at 77, 65, 51 and 39 Da are typical peaks due to fragments formed during the EI ionization of the benzene ring.

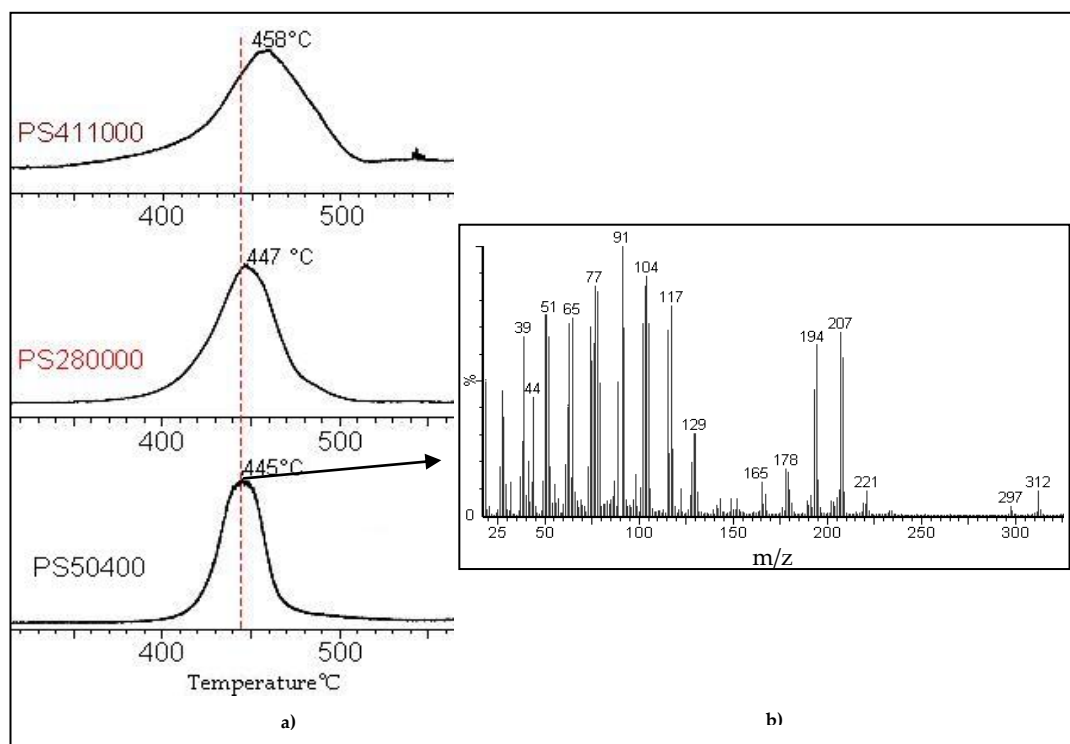


**Figure 3-1:** a) The total ion current (TIC) curve detected during the pyrolysis of PS samples and b) Mass spectrum at 445 °C for PS50400.

**Table 3-1:** The relative intensities (RI) and assignments made for the intense and/or characteristic peaks present in the pyrolysis mass spectrum (Py-MS) of PS50400 at 445 °C.

<b>m/z</b>	<b>RI</b>	<b>ASSIGNMENT</b>
39	680	C <sub>3</sub> H <sub>3</sub>
51	776	C <sub>4</sub> H <sub>3</sub>
65	745	C <sub>5</sub> H <sub>5</sub>
77	854	C <sub>6</sub> H <sub>5</sub>
78	840	C <sub>6</sub> H <sub>6</sub>
<b>91</b>	<b>1000</b>	<b>C<sub>7</sub>H<sub>7</sub></b>
104	898	Styrene (St) Monomer(M)
117	782	MCH
194	640	MCH C <sub>6</sub> H <sub>5</sub>
207	684	[D – H]
208	589	St Dimer (D)
221	83	DCH
312	92	St Trimer (T)
416	1.5	St Tetramer (Te)
520	0.6	St Pentamer (P)

### 3.1.2 Poly(2-vinylpyridine)

In order to investigate thermal degradation mechanism of the poly(2-vinylpyridine) polymer pyrolysis mass spectrometry analysis of two commercial samples with different molecular weights, namely Mw= 11000 and 64000 were performed. TGA analysis of the P2VP polymers indicated that both polymers decomposed totally, just above 400 °C (Figure 3-2).

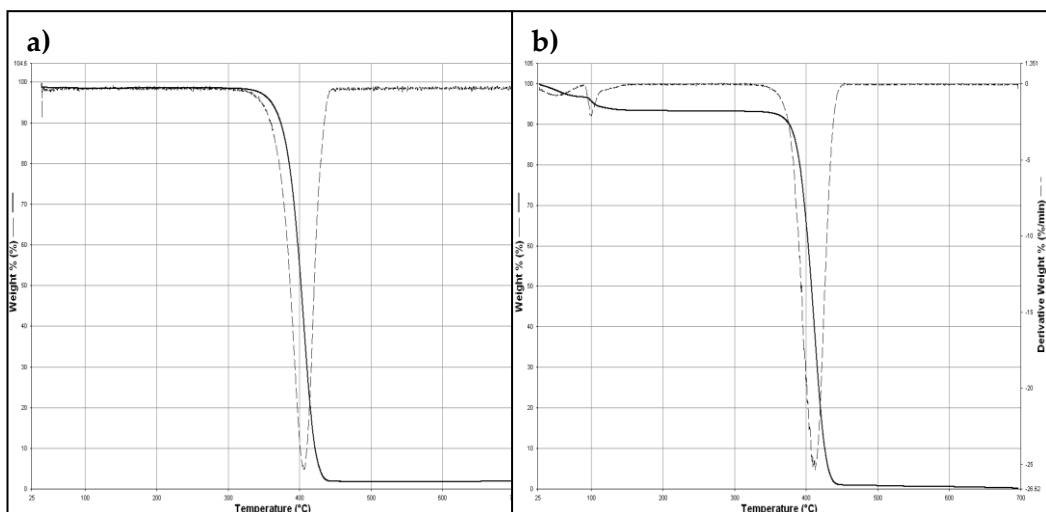


**Figure 3-2:** TGA curves of a) P2VP-1 and b) P2VP-2

Pyrolysis mass spectra of polymers are usually very complex, as thermal degradation products further dissociate in the mass spectrometer during ionization and all fragments with the same mass to charge ratio make contributions to the intensities of the same peaks in the mass spectrum. Thus, interpretation of the spectra is quite difficult. Presence of more than one peak in the TIC curve indicates presence of either a multi-component sample or units with different thermal stabilities. On the other hand, scanning single ion current pyrograms allows separation of decomposition products as a function of volatility and/or thermal stability. Thus, in case of direct pyrolysis MS analyses, not only the detection of a peak but also the variation of its intensity as a function of temperature, i.e. its evolution profile, is important. The trends in evolution profiles can be used to determine the source of the product, or the mechanism of thermal degradation.

### 3.1.2.A P2VP-1 (*M<sub>w</sub>*: 11000)

Pyrolysis mass spectrometry analysis of P2VP-1 indicated that thermal decomposition mainly occurred in the temperature range of 400-500 °C. Figure 3-3 shows the TIC curve and pyrolysis mass spectrum recorded at 435 °C corresponding to peak maximum in the TIC curve.

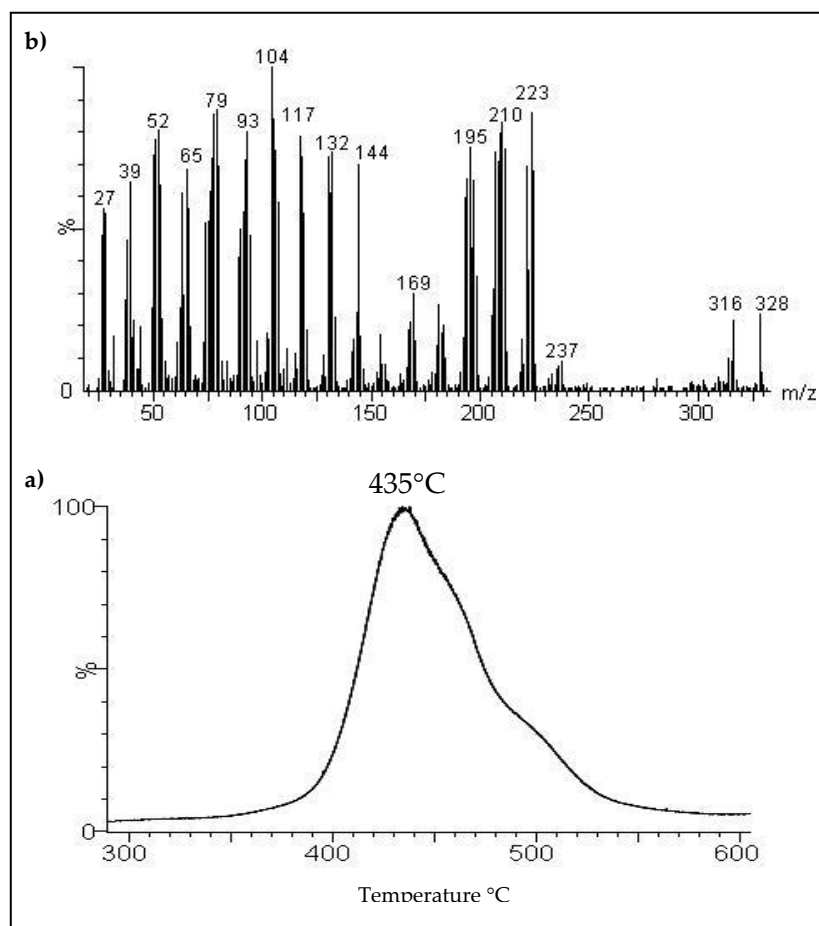


**Figure 3-3:** a) The TIC curve and b) Mass spectrum at 435 °C of P2VP-1

The relative intensities (RI) of the characteristic and/ or intense peaks present in the pyrolysis mass spectrum recorded and the assignments made for both of the P2VP homopolymers are shown in Table 3-2.

**Table 3-2:** RI and assignments made for the intense and/or characteristic peaks present in the (Py-MS) of P2VP-1 Mw: 11000 at 435 °C and P2VP-2 Mw: 64000 at 436 °C

m/z	RI Mw: 11000	RI Mw: 64000	ASSIGNMENT
28	548	463	C <sub>2</sub> H <sub>4</sub>
77	718	733	C <sub>5</sub> H <sub>3</sub> N
78	853	886	C <sub>5</sub> H <sub>4</sub> N
<b>79</b>	867	<b>1000</b>	C <sub>5</sub> H <sub>5</sub> N Pyridine (Py)
91	550	540	C <sub>6</sub> H <sub>5</sub> N
93	799	887	C <sub>6</sub> H <sub>6</sub> NH
<b>104</b>	<b>1000</b>	804	<b>[M - H]</b>
105	840	570	C <sub>7</sub> H <sub>7</sub> N (Vinyl pyridine monomer, M)
106	743	843	MH
118	706	821	MCH
132	738	722	[D - Py]
144	698	648	MC <sub>3</sub> H <sub>3</sub>
195	750	707	[D-CH <sub>3</sub> ]
210	827	899	Dimer (D)
211	745	694	DH
223	858	938	DCH
237	88	116	[T - Py]
315	86	32	Trimer (T)
316	217	251	TH
328	234	371	TCH
342	5.4	7	[Te- Py]
420	7.6	11.2	Tetramer (Te)
421	41.6	78.4	TH
525	1.9	10.1	Pentamer (P)

Inspection of pyrolysis mass spectra indicated generation of monomer and low molecular weight oligomers. Intense peaks due to protonated oligomers were also present. Evolution of monomer (105 Da), dimer (210 Da), trimer (315 Da), tetramer (420 Da) and pentamer (525 Da) generated during the pyrolysis of P2VP-1 were maximized at 435 °C. On the other hand, the yield of protonated monomer and oligomers namely; MH (106 Da), DH (211 Da), TH (316 Da) TeH (421 Da) and PH (526 Da) were maximized or showed a shoulder at around 460°C (Figure 3-4). Another series of product peaks are due to loss of pyridine ring such as [D-Py], [T-Py] and [Te-Py] at  $m/z=$  132, 237, and 342 Da respectively. The evolution profiles of products generated by loss of pyridine showed maxima at 435 °C, but a shoulder at around 460°C was also detected.

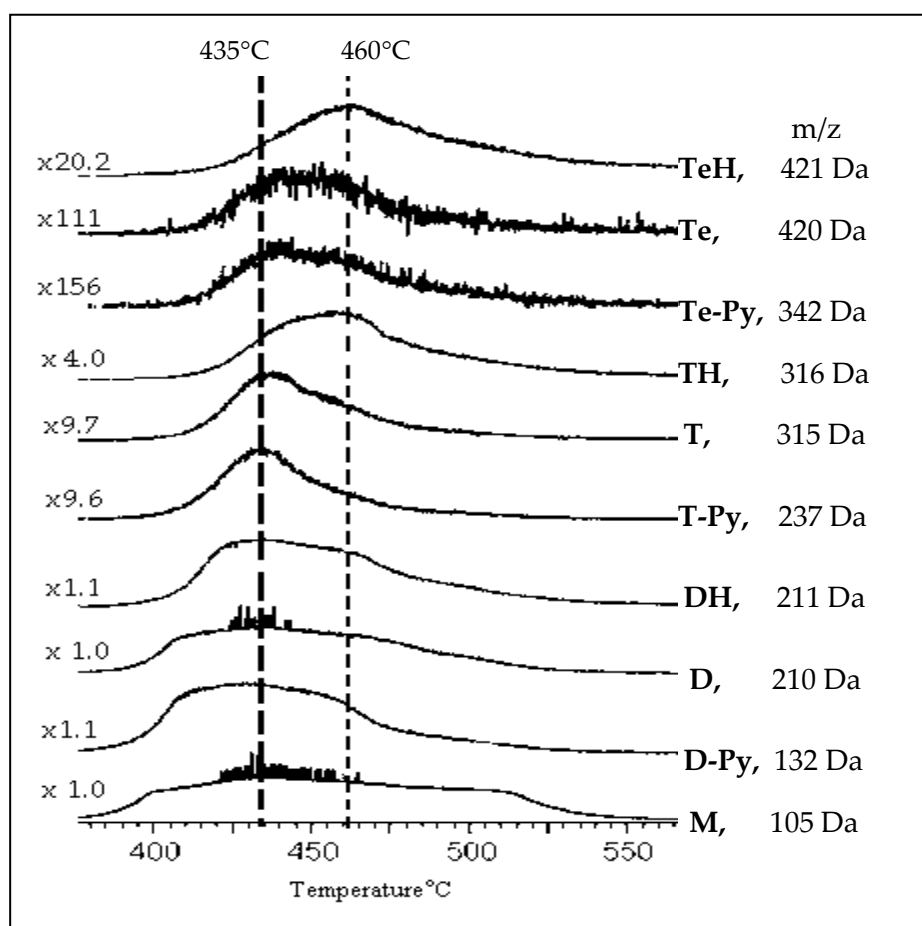
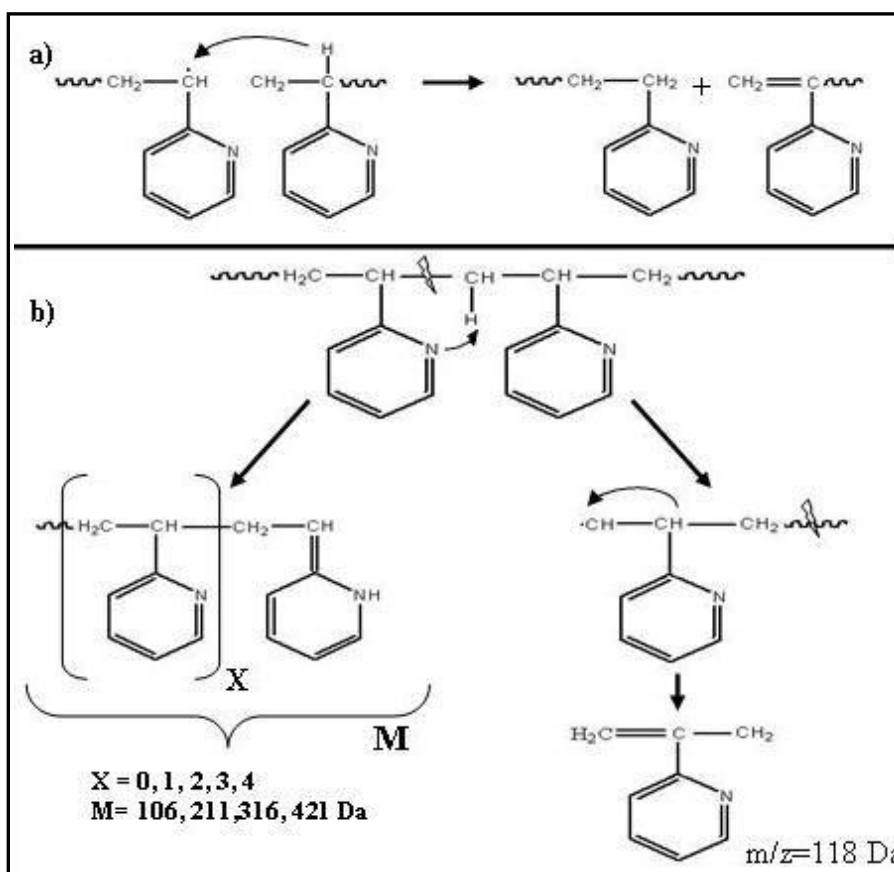


**Figure 3-4:** Pyrograms showing the H transfer and loss of Py ring in P2VP-1

The relative intensities of protonated oligomers were higher than those of the corresponding oligomers, trimer and tetramer. The protonated oligomers may either be generated by H-transfer to the radical chain ends generated by the cleavage of the main chain to increase stability or by H-transfer to N atom on the pyridine ring from the CH<sub>2</sub> groups of the polymer backbone due to the  $\sigma$ -effect before or after thermal degradation as shown in Scheme 3-1. In general, products generated by H-transfer to chain ends show identical evolution profiles with those of the precursors. In our case, the evolution of protonated oligomers was shifted slightly to high temperatures. Thus, it may be thought that the main process was the H-transfer to the N atom on the pyridine ring followed by coupling of the radicals generated on the main chain or double bond formation by further H-transfer reactions.



**Scheme 3-1:** Hydrogen transfer **a)** Inter chain **b)** Intra chain to the N atom.

### 3.1.2.A P2VP-2 ( $M_w$ : 64000)

Pyrolysis mass spectrometry analysis indicated that thermal decomposition of P2VP-2 mainly occurred in the temperature range of 400-500 °C. The TIC curve and the pyrolysis mass spectrum recorded at peak maximum are shown in Figure 3-5.

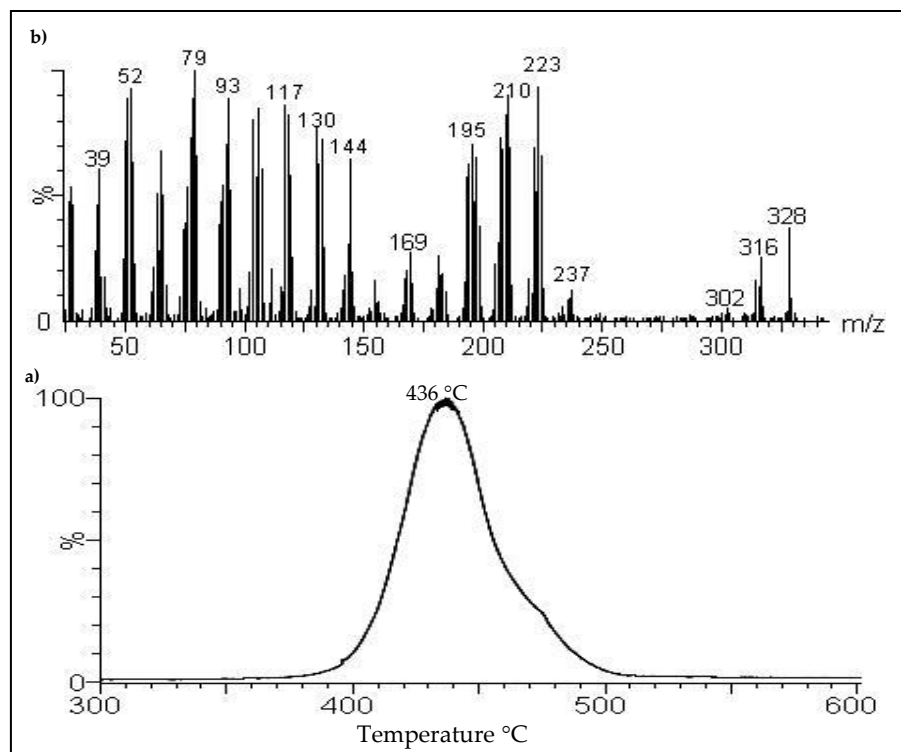


**Figure 3-5:** a) The TIC curve for P2VP and b) Mass spectrum at 436 °C of P2VP-2

The related data are also included in Table 3-2 for comparison and the evolution profiles of characteristic products are shown in Figure 3-6. Note that, for P2VP-2 the yield of monomer and oligomers were also maximized at 436 °C.

Similar degradation products were identified as expected. In Figure 3-6 (a) evolution profiles of oligomers and protonated oligomers generated during the pyrolysis of P2VP-2 are shown. The corresponding ones detected during the

pyrolysis of P2VP-1 (Figure 3-6 (b)) are also included for comparison. For this sample, oligomer peaks were maximized at around 436 °C and protonated oligomers showed maxima at 470 °C, indicating a 34 °C temperature shift. This value is very close to 30 °C temperature shift observed for P2VP-1 polymer. Furthermore, again, as the repeating unit present in the oligomer increased, the ratio of the relative intensities of the protonated oligomers to that of corresponding oligomers also increased. Thus, the trends observed in the pyrolysis mass spectra and in the evolution profiles of the P2VP-1 and P2VP-2 polymers were quite similar.

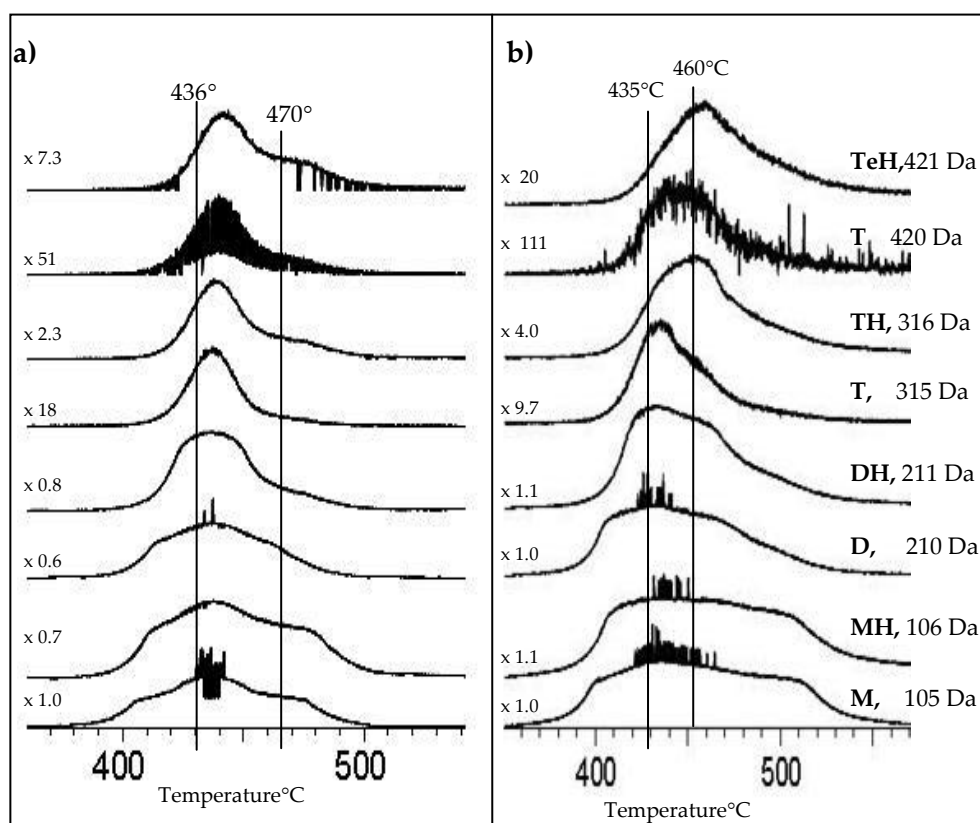
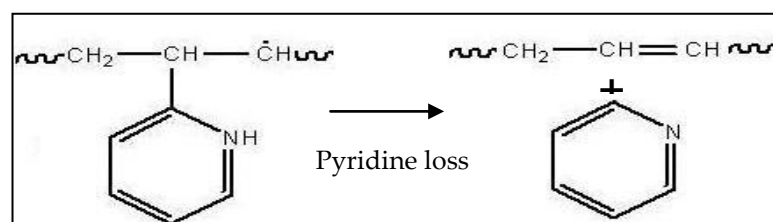


**Figure 3-6:** Comparison of single ion pyrograms for a) P2VP-2 and b) P2VP-1 polymers

In case of PS, with almost a similar structure with P2VP except the N in the ring, peaks due to protonated oligomers or loss of phenyl group were almost absent.

Thus, it can be concluded that the thermal degradation of P2VP occurs through different decomposition pathways. In general, the mechanism of the thermal decomposition of vinyl polymers is depolymerization reactions yielding mainly monomer and low mass oligomers. However, the data indicated that for P2VP, besides the protonated oligomer peaks, peaks generated by the loss of  $C_5H_4N$  (Py) and  $C_6H_5N$ , such as D-Py peak at 132, are also quite intense. The proposed mechanism of pyridine loss is shown in Scheme 3-2.



**Scheme 3-2:** Possible mechanism for the loss of pyridine

Thus, it can be concluded that thermal degradation of P2VP occurs by opposing reactions as;

- Depolymerization yielding mainly monomer and low molecular weight oligomers,
- Proton transfer to N atom yielding unsaturated linkages on the polymer backbone which in turn increases thermal stability.
- Loss of pyridine.

### 3.1.3 Poly (4-vinylpyridine)

The TGA analysis indicated that weight loss of P4VP was 100% at 413 °C (Figure 3-7)

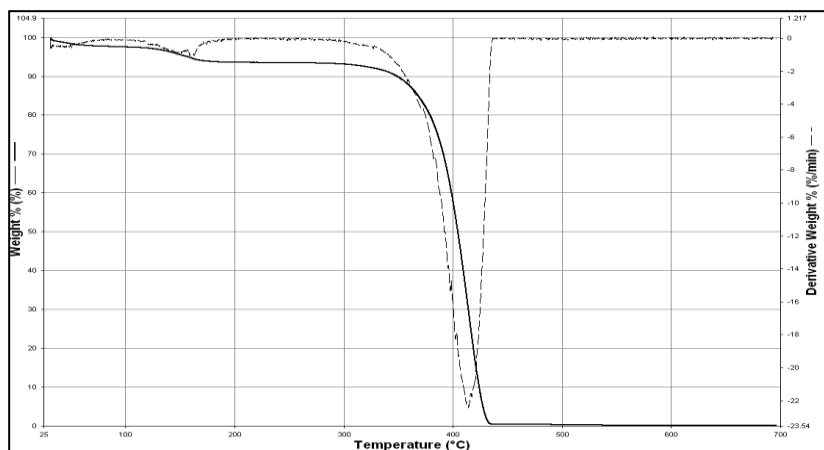


**Figure 3-7:** TGA curve for P4VP

The TIC curve and the pyrolysis mass spectrum recorded at the peak maximum at 433 °C recorded during the pyrolysis of P4VP are shown in Figure 3-8.

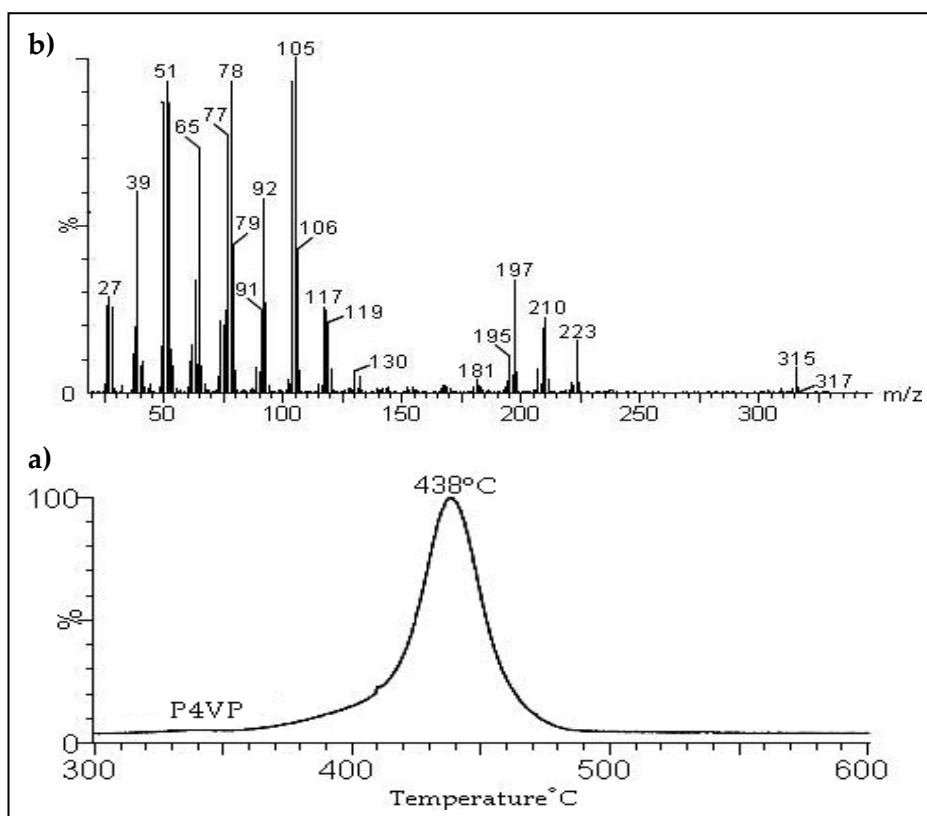


**Figure 3-8:** a) TIC curve and b) Spectrum of P4VP homopolymer at 438 °C

The base peak was at 105 Da due to the monomer. The relative intensities of the peaks at  $m/z > 105$  Da were quite low. It can be noted that, thermal degradation of P4VP occurred in a temperature range very similar to that of P2VP, but the thermal degradation products and their relative yields were somewhat different. The relative intensities of peaks due to protonated oligomers and loss of pyridine units were significantly diminished yielding less crowded pyrolysis mass spectra. The main reason for this behavior is, most probably, the absence of hydrogen transfer reactions to nitrogen atom which is at para position in P4VP sample. The relative intensities of intense and/or characteristic peaks present in the pyrolysis mass spectrum of P4VP recorded at 433 °C and the assignments made are collected in Table 3-3. Note that the relative intensities of the peaks due to loss of pyridine and protonated oligomers are significantly lower than those of P2VP. The significant decrease in the relative intensities of peaks due to products generated by loss of pyridine from dimer, trimer and tetramer at  $m/z=132$ , 237 Da and 342 Da respectively pointed out that, pyridine loss is not a favored pathway for thermal degradation of P4VP polymer. The decrease in the relative yields of protonated oligomers is in accordance with general expectations; hydrogen transfer to nitrogen in para position is not favored in P4VP. The decrease in relative intensities of peaks due to protonated oligomers and loss of pyridine units pointed out that loss of pyridine detected during the pyrolysis of P2VP samples mainly occurred after proton transfer to N as shown in Scheme 3-2.

All products showed almost identical trends in their single ion pyrograms. In Figure 3-9 evolution profiles of monomer, dimer, trimer, protonated dimer and trimer are shown. Thus, it can be concluded that thermal degradation of P4VP occurs by;

- Depolymerization yielding mainly monomer and low mass oligomers as in case of most of the vinyl polymers.

**Table 3-3:** Peak assignments of P4VP polymer

m/z	RI at 438 °C	ASSIGNMENT
28	256	C <sub>2</sub> H <sub>4</sub>
77	768	C <sub>5</sub> H <sub>3</sub> N
78	931	C <sub>5</sub> H <sub>4</sub> N
79	442	C <sub>5</sub> H <sub>5</sub> N (Py)
91	246	C <sub>6</sub> H <sub>5</sub> N
92	581	CH <sub>2</sub> + C <sub>5</sub> H <sub>4</sub> N, C <sub>7</sub> H <sub>8</sub>
104	930	C <sub>7</sub> H <sub>7</sub> N - H
<b>105</b>	<b>1000</b>	<b>C<sub>7</sub>H<sub>7</sub>N (Monomer, M or VP)</b>
106	428	MH
117	256	132- CH <sub>3</sub>
132	45.6	D - C <sub>5</sub> H <sub>4</sub> N
144	17.6	223-Py
195	109	104 + 91
210	225	Dimer (D)
211	37.4	DH
223	156	T - C <sub>6</sub> H <sub>6</sub> N
237	5.3	T - C <sub>5</sub> H <sub>4</sub> N
315	73	Trimer (T)
316	16.1	TH
328	2.7	TCH
342	0.2	Te - C <sub>5</sub> H <sub>4</sub> N
420	0.8	Tetramer (T)
421	0.5	TH

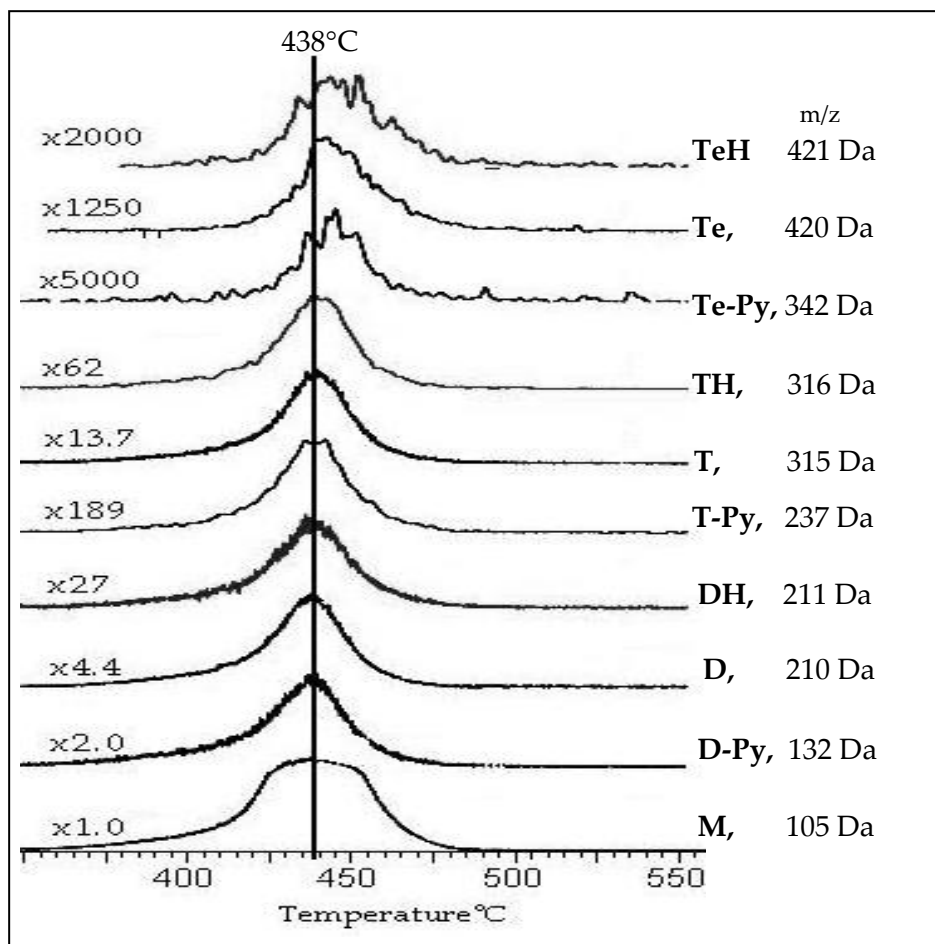
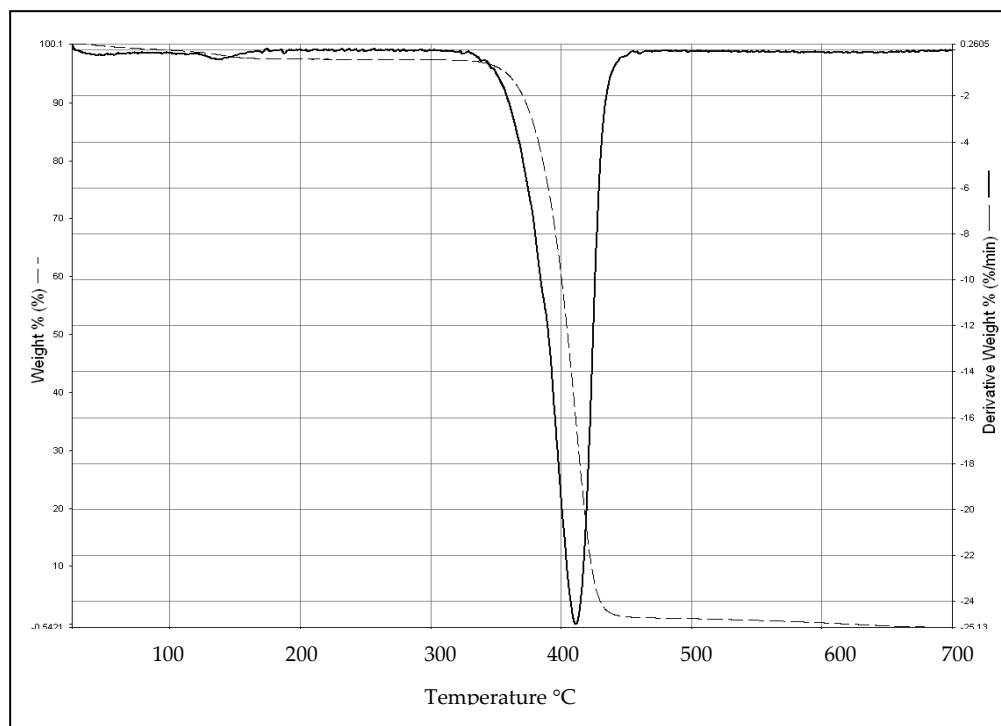


Figure 3-9: P4VP pyrograms showing the lack of hydrogen transfer to N atom.

## 3.2 PYROLYSIS OF DIBLOCK COPOLYMERS

### 3.2.1 PS-b-P2VP Diblock Copolymer

TGA results indicated that the polymer degrades completely and the degradation of the copolymer occurs at around 415 °C (Figure 3-10).



**Figure 3-10:** TGA results for the PS-b-P2VP

Direct pyrolysis mass spectrometry studies (Figure 3-12) showed a TIC curve with a maximum at 433 °C, 18 °C higher than the corresponding value of TGA. In general, it is known that TGA and DP-MS data are quite similar, and this slight difference can be attributed to sampling.

As previously stated, the mass spectral data for the PS homopolymer showed that molecular weight, in the range studied, have no significant effect on the thermal degradation behavior of PS. Similar studies were also performed for PS-b-P2VP diblock copolymers having variable compositions.

The TIC curves of the diblock copolymers having different compositions are shown in Figure 3-11. On the right the TIC curves of the polymers synthesized by Hadjichristidis, N. were arranged according to percent weight of PS increased in the order S7<S6<S5<S4<S3. Actually, except S7 molecular weight of the diblock

copolymer also increased in the same order. On the left, the TIC curves of the copolymers PS-b-P2VP-1 and PS-b-P2VP-2, involving P2VP blocks with almost identical molecular weights but PS blocks with molecular weights 58000 and 25000 were shown.

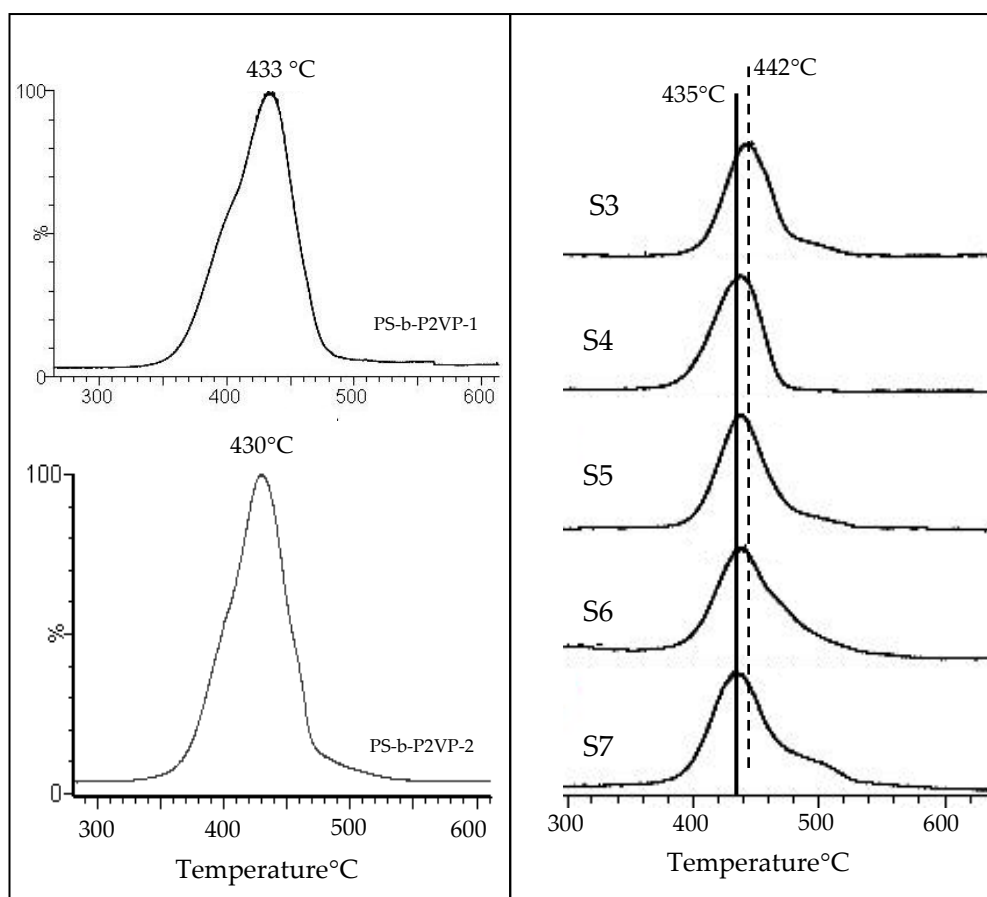


**Figure 3-11:** The effect of composition change in the PS-b-P2VP diblock copolymers.

Note that, only a slight shift to higher temperatures with increase in molecular weight was detected. Thus, it can be concluded that the change in composition or molecular weight in the ranges studied does not have a significant effect on the thermal stability of the PS-b-P2VP diblock polymer. Furthermore, pyrolysis mass spectra of all the samples were dominated with identical peaks indicating that not

only thermal stability but also thermal degradation mechanism were independent of the composition and molecular weight of the sample in the range studied. The only difference was the variations in the relative intensities of the peaks; as the PS content increased the relative intensities of the relative peaks increased.

### 3.2.1.A PS-*b*-P2VP-1

In Figure 3-12, the TIC curve and the pyrolysis mass spectra at 433 °C and 399 °C, the peak maximum and the shoulder present in the TIC curve, recorded during the pyrolysis of PS-*b*-P2VP-1 are shown. Above 350 °C, generation of series of fragments such as  $M_x$ ,  $[M_x-CH_2]$ ,  $[M_x-CH]$ ,  $M_xCH$ ,  $M_xCH_2$ ,  $M_xC\equiv CH$ ,  $M_xCH=CH_2$  where M is either  $C_6H_5$  or  $C_5H_4N$  and  $x = 1, 2, 3,$  or  $4$  were observed. Peaks due to fragments stabilized by hydrogen exchange reactions were also detected.

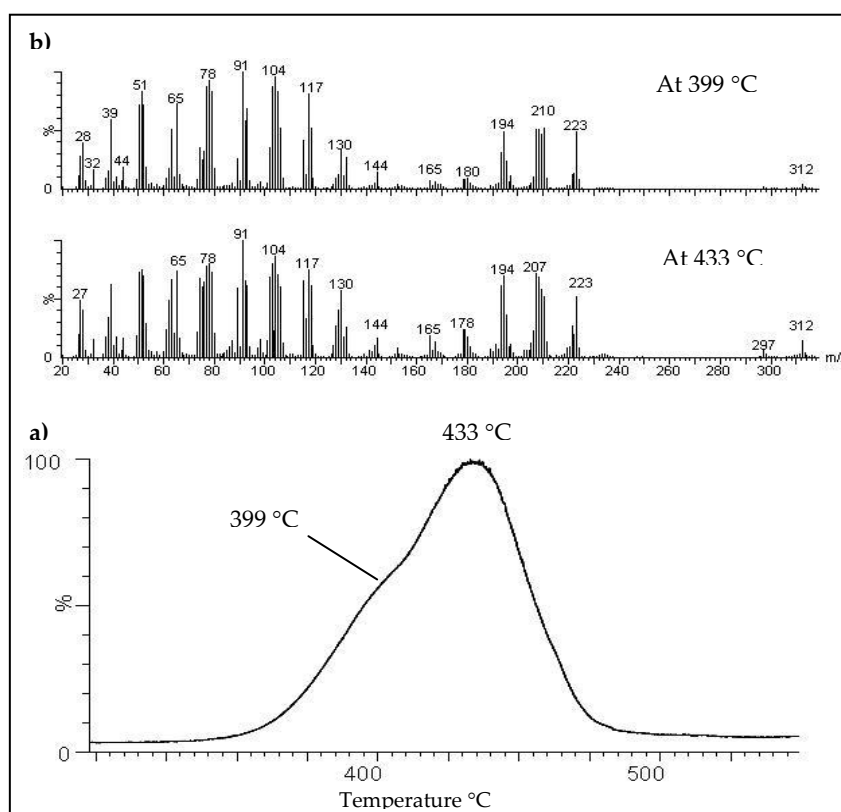


**Figure 3-12:** a) The TIC Curve and b) Pyrolysis mass spectra recorded for PS-*b*-P2VP-1.

The characteristic peaks of PS were relatively more intense than those of P2VP in the pyrolysis mass spectra of the block copolymer as expected considering the composition of the diblock copolymer. For instance, the base peak for the diblock copolymer was at  $m/z=91$  Da due to  $C_7H_7$ , similar to what was observed in the pyrolysis mass spectra of PS homopolymer. Peaks due to styrene (St) and 2-vinylpyridine (VP) monomers and low mass oligomers are among the most intense.

The relative intensities of intense and/or characteristic peaks and the assignments made are collected in Table 3-4. To get a better understanding of the degradation mechanism of the diblock copolymer, evolution of products associated with P2VP and PS blocks were identified and compared. The single ion pyrograms of some selected products are shown in Figure 3-13. The trends in the evolution profiles indicated a lower thermal stability for P2VP block compared to PS blocks. It is clear that both of the components degraded independently. Thermal degradation products of P2VP block were maximized at 428 °C, at lower temperatures than those of the PS block that were maximizing at 437 °C.

The evolution profiles of protonated oligomers of P2VP again showed maxima at higher temperatures, compared to the corresponding oligomers, around 441 °C. Furthermore, protonated trimer and tetramer peaks of P2VP were more intense than the corresponding oligomers as in case of the homopolymer. Thus, it can be concluded that each component decomposed independently through similar decomposition pathways proposed for the corresponding pure homopolymers.

**Table 3-4:** Peak assignments of PS-b-P2VP diblock copolymer

m/z	RI. at 428 °C	RI At 437 °C	ASSIGNMENT
91	1000	1000	C <sub>7</sub> H <sub>7</sub> , C <sub>6</sub> H <sub>5</sub> N
104	177	870	St, C <sub>8</sub> H <sub>8</sub> , [VP-H]
105	728	692	StH, VP
116	302	351	(C <sub>6</sub> H <sub>5</sub> )CH=C=CH <sub>2</sub> ,
117	745	714	(C <sub>6</sub> H <sub>5</sub> )CH-CH=CH <sub>2</sub> , (C <sub>5</sub> H <sub>4</sub> N)CH=C=CH <sub>2</sub>
118	636	593	(C <sub>5</sub> H <sub>4</sub> N)CH-CH=CH <sub>2</sub> , StCH <sub>2</sub>
129	346	455	StC≡CH
130	590	558	PVC≡CH
165	165	182	C <sub>13</sub> H <sub>8</sub> ,
178	217	244	C <sub>15</sub> H <sub>11</sub>
179	210	232	C <sub>15</sub> H <sub>12</sub>
194	695	676	[St <sub>2</sub> – CH <sub>2</sub> ]
207	733	721	[St <sub>2</sub> – H]
208	692	675	St <sub>2</sub> Dimer
210	600	419	VP <sub>2</sub> - Dimer
211	149	115	VP <sub>2</sub> H
221	261	253	St(C <sub>6</sub> H <sub>5</sub> )CH-CH=CH <sub>2</sub> , VP(C <sub>5</sub> H <sub>4</sub> N)C=C=CH <sub>2</sub>
223	611	425	VP <sub>2</sub> (CH) St <sub>2</sub> CH <sub>3</sub>
312	126	148	St <sub>3</sub> Trimer
315	11.5	8.6	VP <sub>3</sub> Trimer
316	14.5	17.6	VP <sub>3</sub> H
416	2.1	3.6	St <sub>4</sub> Tetramer,
420	0.8	0.5	VP <sub>4</sub> Tetramer
421	2.9	4.5	VP <sub>4</sub> H

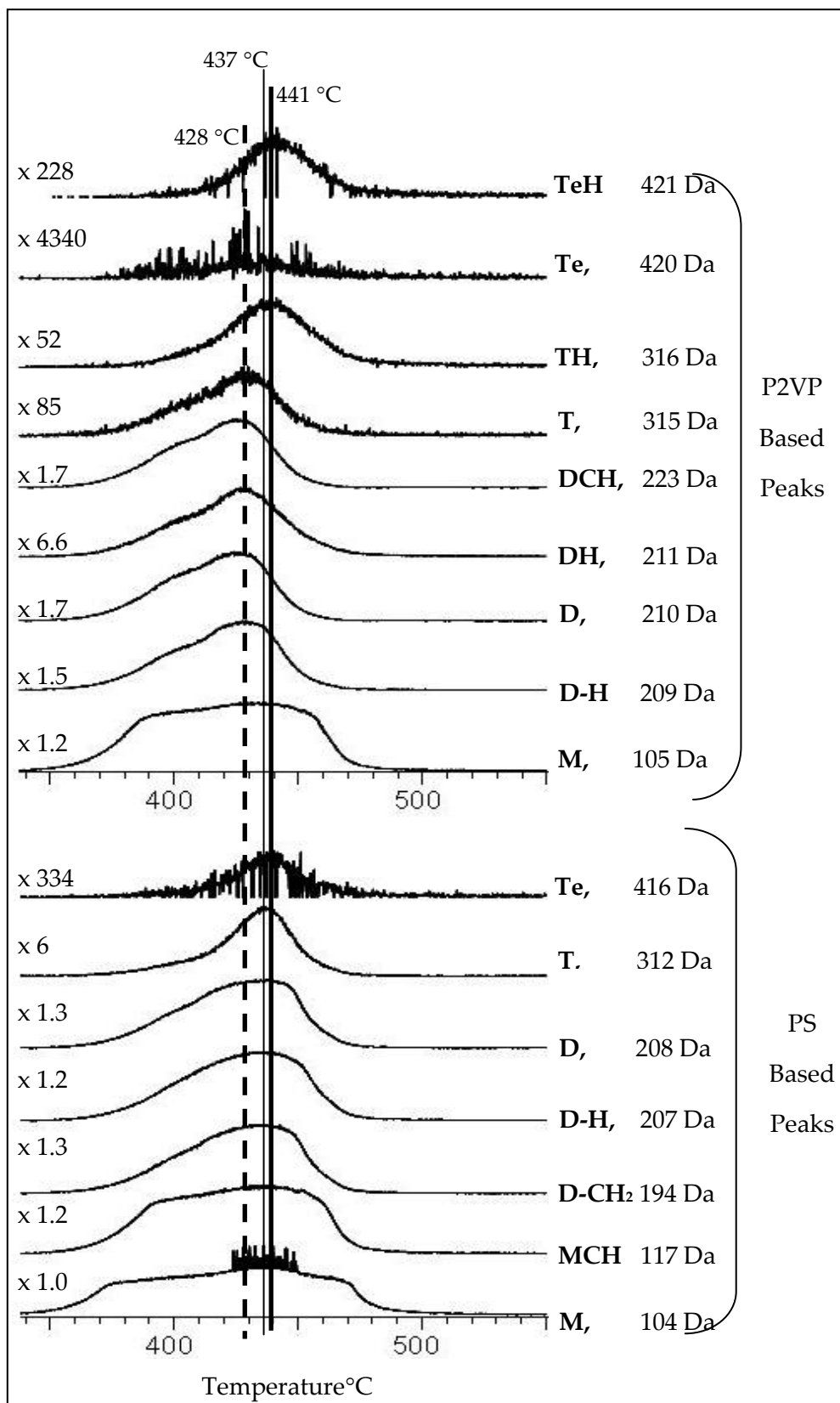
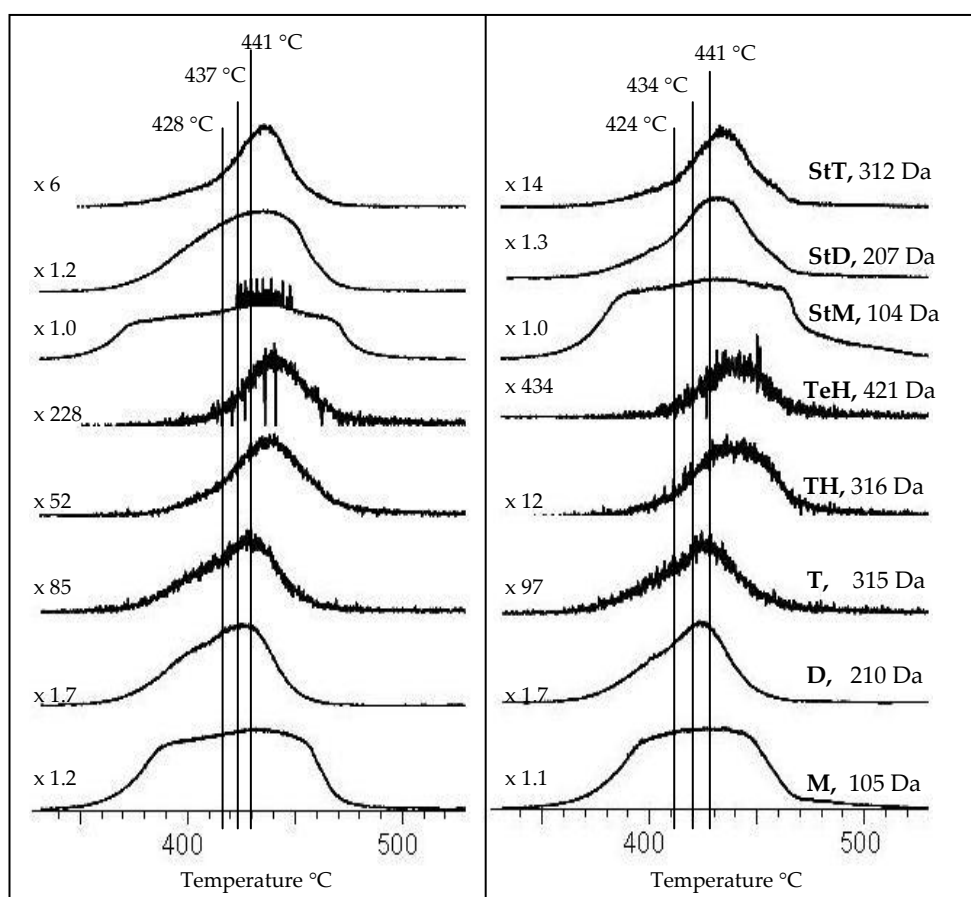


Figure 3-13: Single ion pyrograms of some selected products of PS-b-P2VP-1

### 3.2.1.A PS-*b*-P2VP-2

The copolymer sample PS-*b*-P2VP-S2 (25000/15000) showed almost an identical behavior, yet, relative intensities of PS based products decreased as expected. In Figure 3-14, evolution profiles of styrene and styrene dimer and trimer, 2-vinylpyridine, 2-vinylpyridine dimer, and trimer, and corresponding protonated oligomers recorded during the pyrolysis of PS-*b*-P2VP-1 and PS-*b*-P2VP-2 are shown for comparison. Note that, during the pyrolysis of PS-*b*-P2VP-2, oligomers of 2-vinylpyridine, styrene and protonated oligomers of 2-vinylpyridine were maximized at 424 °C, 434 °C and 441 °C respectively. As expected, a slight decrease in thermal stability compared to PS-*b*-P2VP-1 was detected.



**Figure 3-14:** Comparison of a) PS-*b*-P2VP-1 and b) PS-*b*-P2VP-2 copolymers.

### 3.2.2 PS-b-P4VP Diblock Copolymer

In order to investigate the effect of the position of the nitrogen atom in the pyridine ring, thermal degradation behavior of P4VP copolymer was also investigated. TGA results indicated that the PS-b-P4VP copolymer degrades completely and the degradation of the copolymer occurs at around 415 °C (Figure 3-15).

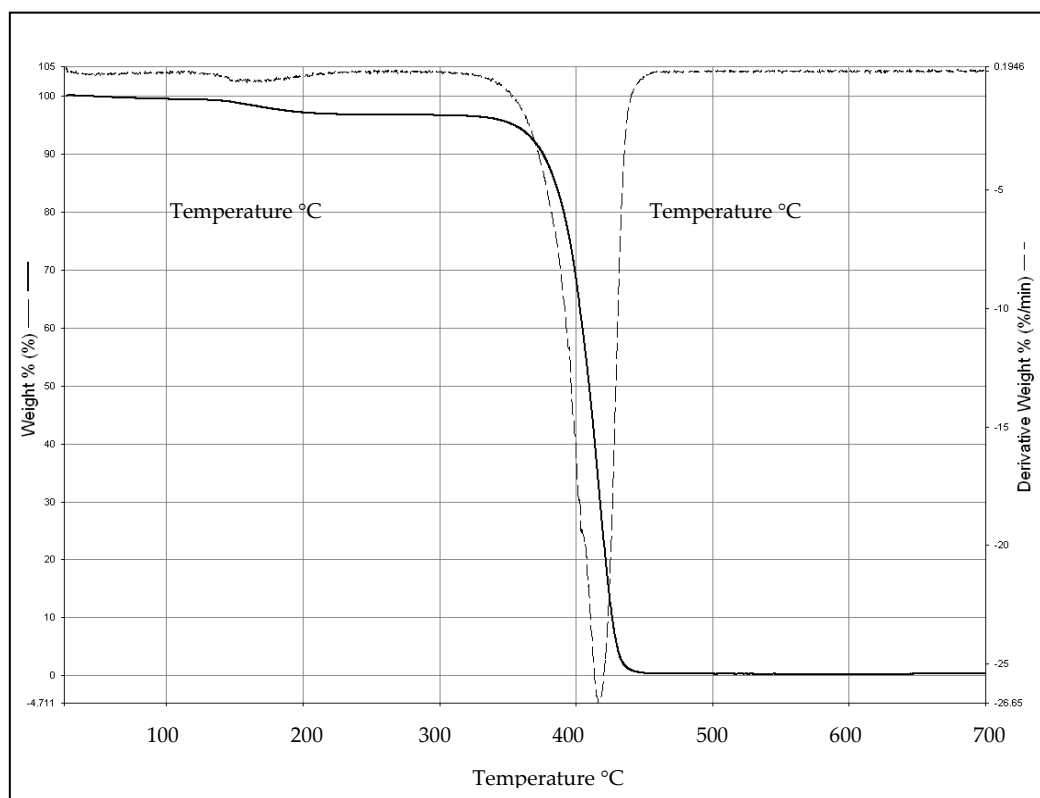


**Figure 3-15:** TGA for PS-b-P4VP copolymer

Direct pyrolysis mass spectrometry analysis of PS-b-P4VP diblock copolymer yielded a TIC curve with two well separated peaks. The TIC curve and the pyrolysis mass spectra recorded at the peak maxima are shown in Figure 3-16.

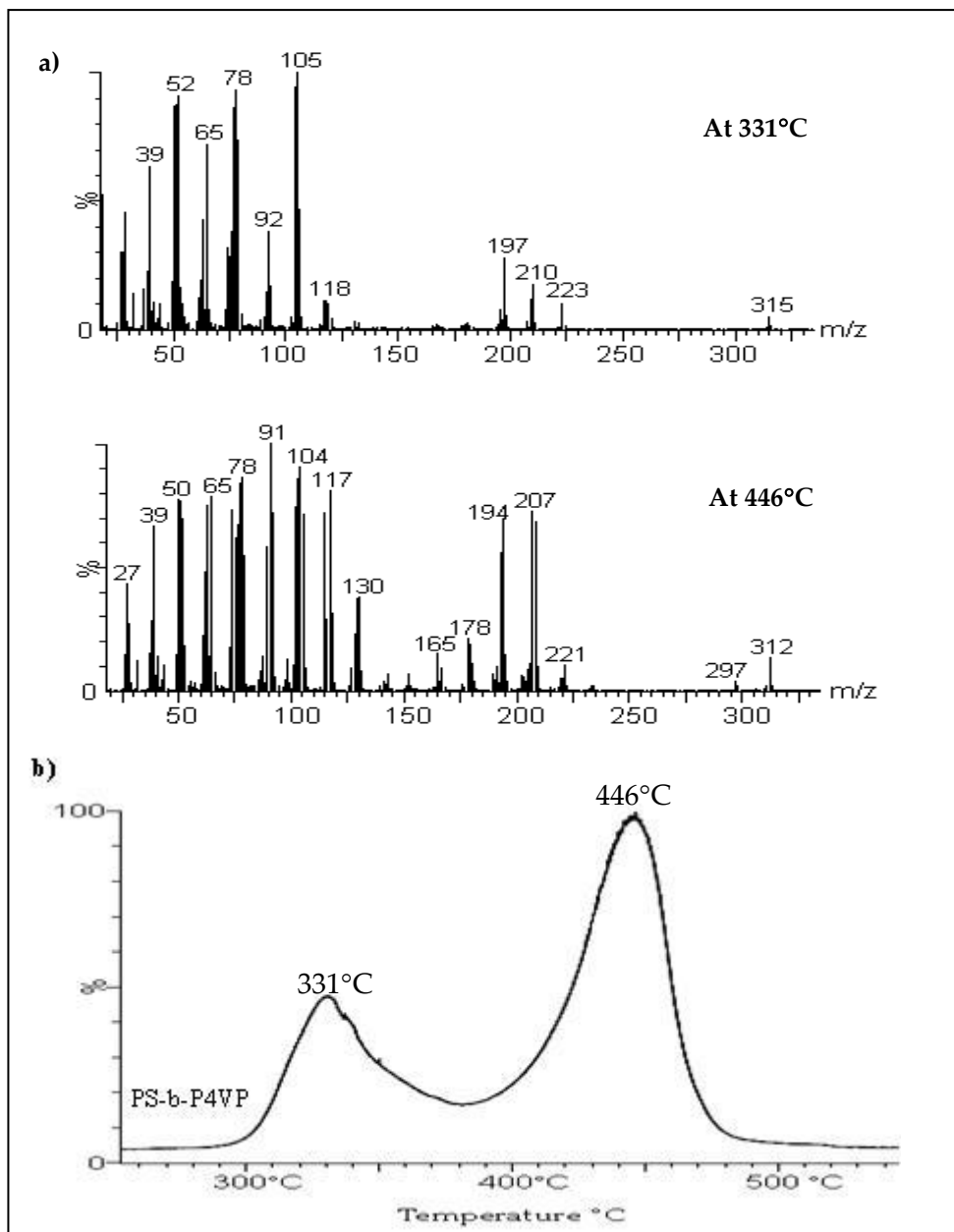


**Figure 3-16:** a) The TIC curve and b) Spectrum at two maxima for PS-b-P4VP polymer

Table 3-5 shows the relative intensities and the assignments made for the intense and/or characteristic peaks for the PS-b-P4VP diblock copolymer.

**Table 3-5:** Peak assignments for PS-b-P4VP polymer

m/z	RI at 331 °C	RI at 446 °C	ASSIGNMENT
<b>91</b>	143	<b>1000</b>	<b>C<sub>7</sub>H<sub>7</sub>, C<sub>6</sub>H<sub>5</sub>N</b>
104	946	839	St, C <sub>8</sub> H <sub>8</sub> , [VP-H]
<b>105</b>	<b>1000</b>	708	StH, VP
117	110	795	(C <sub>6</sub> H <sub>5</sub> )CH-CH=CH <sub>2</sub> , (C <sub>5</sub> H <sub>4</sub> N)CH=C=CH <sub>2</sub>
118	119	309	(C <sub>5</sub> H <sub>4</sub> N)CH-CH=CH <sub>2</sub> , StCH <sub>2</sub>
129	6	373	StC≡CH
130	29	376	VPC≡CH
165	11	149	C <sub>13</sub> H <sub>8</sub> ,
178	9.6	203	C <sub>15</sub> H <sub>11</sub>
194	22.1	685	[St <sub>2</sub> – CH <sub>2</sub> ]
195	72	148	[St <sub>2</sub> – CH], [VP <sub>2</sub> – CH <sub>3</sub> ]
207	33	713	[St <sub>2</sub> – H]
208	8.1	666	St <sub>2</sub> Dimer
209	125	103	St <sub>2</sub> H, [VP <sub>2</sub> – H]
210	161	11	VP <sub>2</sub> Dimer
211	25	2.6	VP <sub>2</sub> H
221	15.6	106	St(C <sub>6</sub> H <sub>5</sub> )CH-CH=CH <sub>2</sub> , P(C <sub>5</sub> H <sub>4</sub> N)C=C=CH <sub>2</sub>
223	101	3	VP <sub>2</sub> (CH) St <sub>2</sub> CH <sub>3</sub>
312	0.5	130	St <sub>3</sub> Trimer
315	53	1.1	VP <sub>3</sub> Trimer
316	8	0.3	VP <sub>3</sub> H
416	0	1.6	St <sub>4</sub> Tetramer
420	0.1	0.1	VP <sub>4</sub> Tetramer
421	0.1	0.1	VP <sub>4</sub> H

The results showed that again both components degraded independently, P4VP being the thermally less stable one. The yield of P4VP based products maximized at 331 °C, about 121 °C lower than the corresponding value detected for P4VP homopolymer (438 °C) and about 100 °C lower than the corresponding value detected for P2VP blocks of the copolymer (428 °C). This decrease compared to P4VP homopolymer may be attributed to the decrease in molecular weight of P4VP block in the block copolymer. The molecular weights of P2VP and P4VP in the block copolymer were comparable. Thus, it may be thought that, in this case the decrease in thermal stability is mainly due to the position of the N atom in the pyridine ring, lack of H transfer reactions. The single ion pyrograms of some characteristic products for both of the components are shown in Figure 3-17.

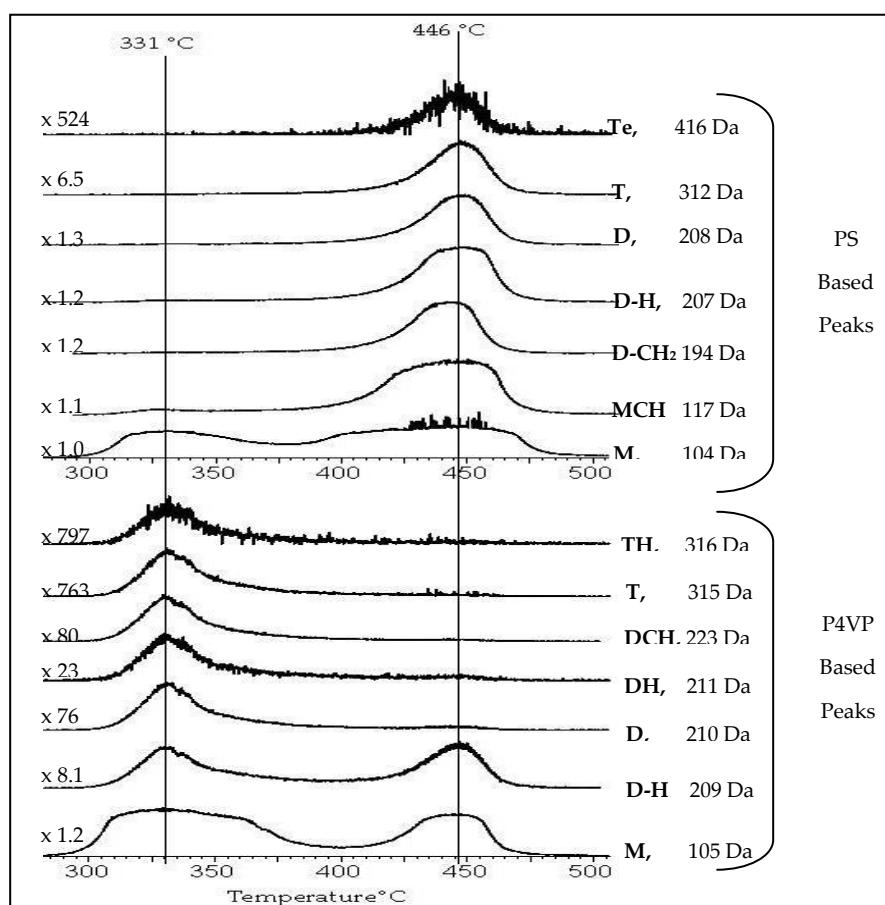


Figure 3-17: Single ion pyrograms of some selected products of PS-b-P4VP

### 3.3. METAL FUNCTIONAL POLYMERS

In order to investigate the effects of Co metal on thermal behavior of the block copolymers, direct pyrolysis mass spectrometry analysis of copolymers refluxed in toluene under the same experimental conditions in the absence of  $\text{Co}_2\text{CO}_8$  were performed.

The TIC curve and pyrolysis mass spectrum of the refluxed copolymer are shown in Figure 3-18 along with the corresponding non refluxed sample. The TIC curves and the pyrolysis mass spectra for both polymers are almost the same. This result pointed out that, refluxing for 8 hours in toluene did not have any significant effect on the thermal behavior of the copolymer.

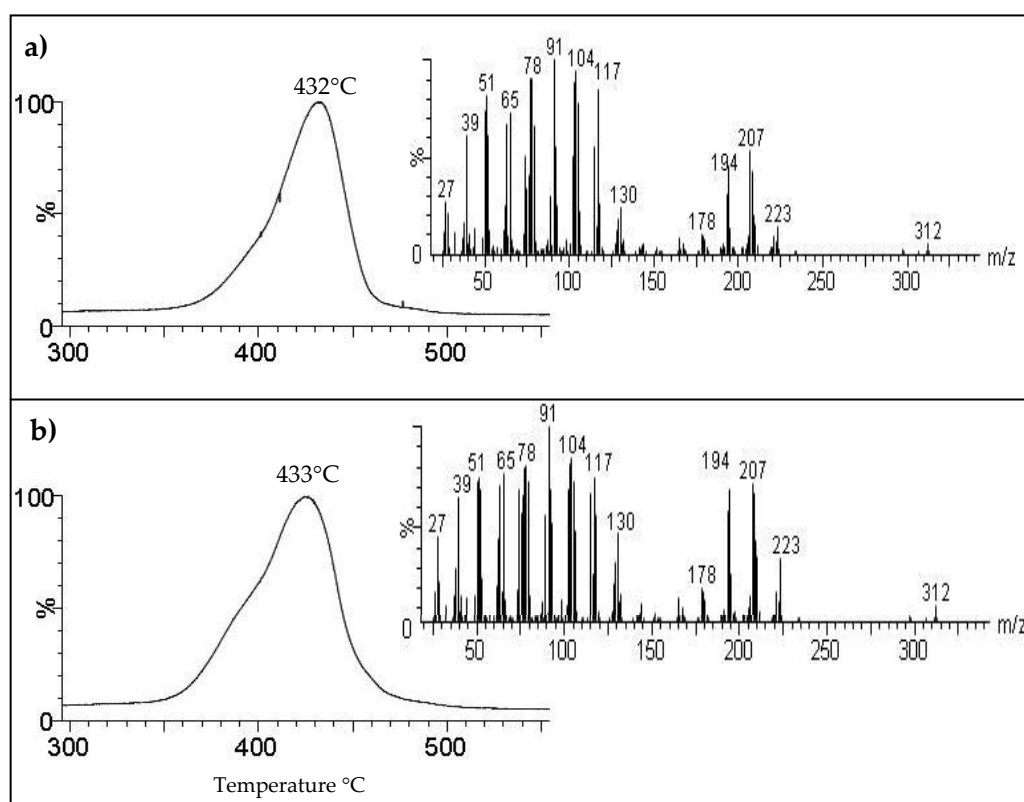
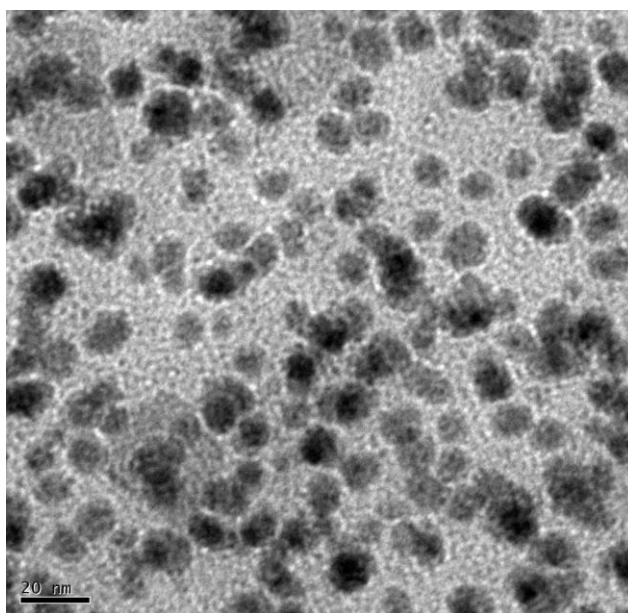


Figure 3-18: TIC curve and spectrum for a) Refluxed PS-b-P2VP and b) PS-b-P2VP

### 3.2.3 Cobalt-PS-b-P2VP Diblock Copolymer

In order to determine the distribution of metal atoms in the polymer matrices TEM images of the metal functional polymers were obtained. Figure 3-19 shows well dispersed cobalt nanoparticles in PS-b-P2VP matrix. Thus, TEM image of PS-b-P2VP confirms metal coordination to nitrogen atom.



**Figure 3-19:** TEM image for Co-PS-b-P2VP polymer

TGA results indicated that the degradation of the Co-PS-b-P2VP copolymer occurred in a broad temperature range and maximum decomposition took place at around 445 °C. It was also seen that 32.5% of the copolymer did not thermally degrade (Figure 3-20) unlike the copolymer. Actually, this is an expected behavior as the sample contained metal particles.

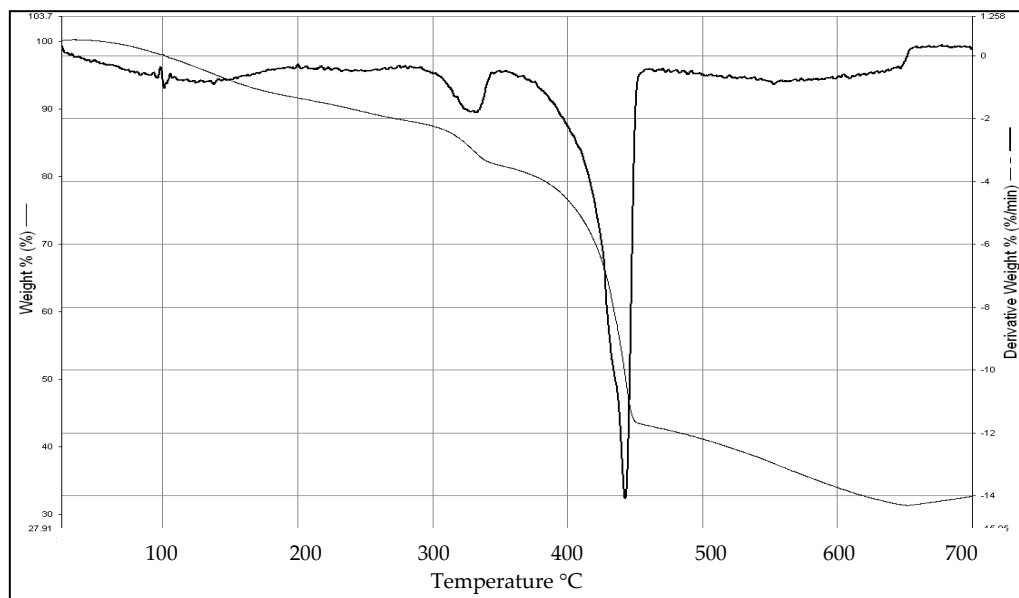


**Figure 3-20:** TGA of the Co-PS-b-P2VP organometallic polymer

The TIC curve and the pyrolysis mass spectra at the peak maximum, at 464 °C and at the shoulder, at 418 °C recorded during the pyrolysis of cobalt functional copolymer are shown in Figure 3-21. The degradation temperature for the Co-PS-b-P2VP showed a significant shift to higher degrees compared to the PS-b-P2VP copolymer, indicating a significant increase in thermal stability (Figure 3-22). The relative intensities and the assignments made for the intense and/or characteristic peaks are collected in Table 3-6. Pyrolysis mass spectra recorded around 464 °C showed significant changes in the oligomer peak intensities. But, what is more important was the presence of peaks that were absent or very weak in the pyrolysis mass spectra of PS-b-P2VP.

Cobalt is expected to be bonded to nitrogen atom in the pyridine ring of the P2VP. Therefore, appearance of new peaks in the pyrolysis mass spectra, variations in the relative intensities of the diagnostic peaks of PS-b-P2VP and changes in the single ion pyrograms of characteristic degradation products can directly be attributed to the metal effect.

One may consider that, the strong interaction between the metal and the nitrogen atom in the pyridine rings of P2VP polymer should inhibit the H-transfer reactions and decrease the yield of protonated oligomers. On the other hand as the molecular weight of the side chains increased, the bond connecting pyridine ( $C_5H_4N$ ) to the main chain can be dissociated more readily by abstracting a proton from  $CH_2$  group leaving two adjacent radicals along the main chain. As a result, either a conjugated double bond or a crosslinked structure due to intermolecular coupling reactions between the main chains of P2VP can be formed as shown in Scheme 3-3.

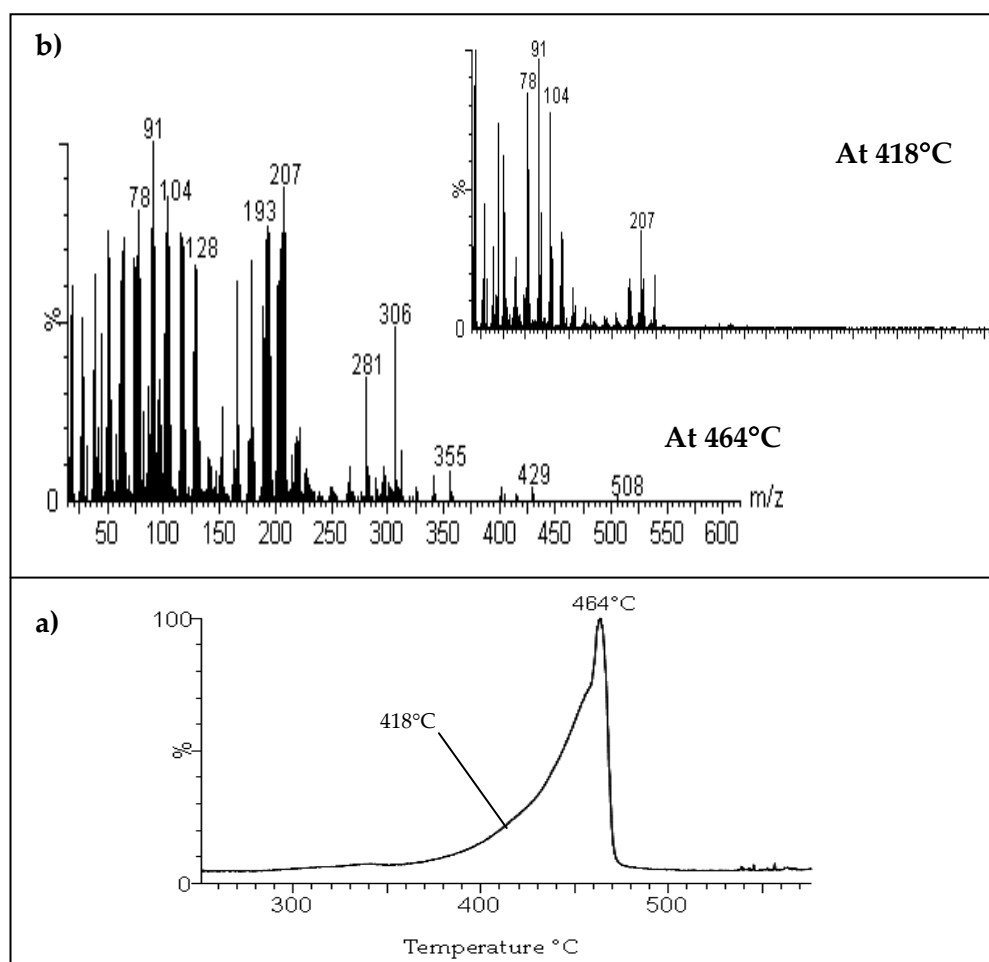


**Figure 3-21:** a) The TIC curve and b) Spectrum at the peak maximum and at the shoulder.

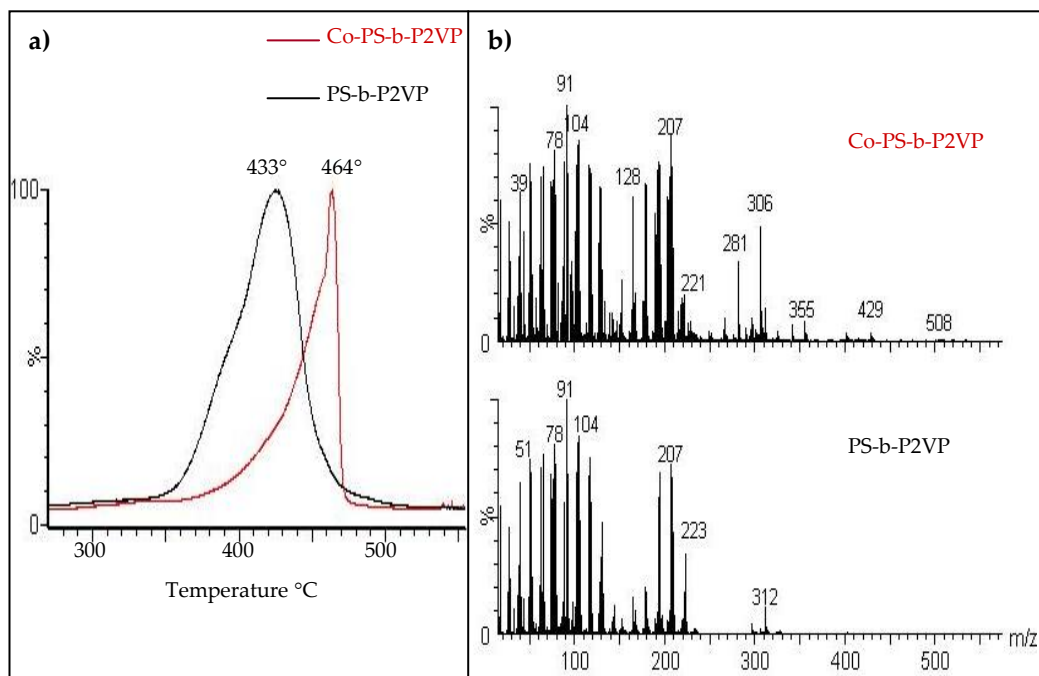
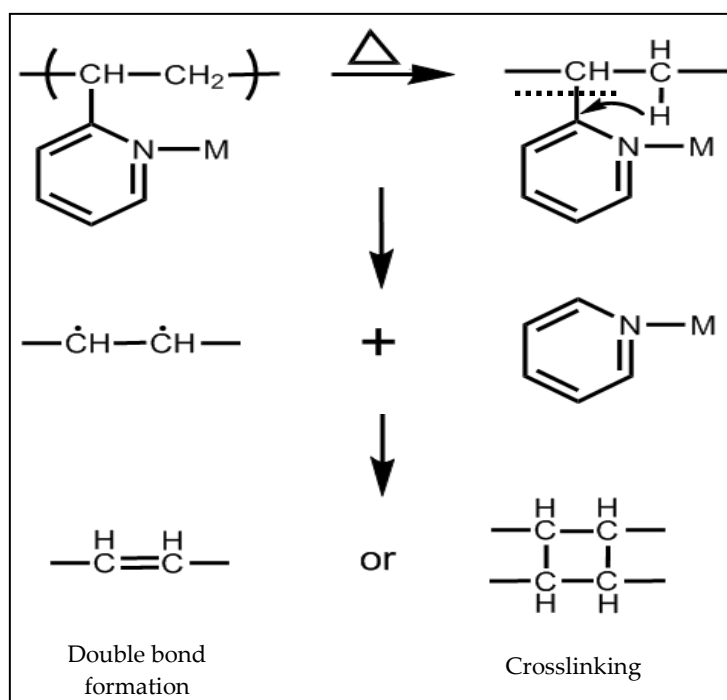


**Figure 3-22:** Comparison of the metal functional polymer with PS-b-P2VP a) TIC curves and b) Pyrolysis mass spectra



**Scheme 3-3:** Possible results of the interaction of metal with the pyridine ring

**Table 3-6:** Peak assignments for Co-PS-b-P2VP

m/z	RI At 418 °C	RI At 464 °C	ASSINGMENT
91	1000	1000	C <sub>7</sub> H <sub>7</sub> , C <sub>6</sub> NH <sub>5</sub>
104	896	850	St, C <sub>8</sub> H <sub>8</sub> , [VP-H]
105	349	706	StH, VP
106	233	210	VPH
117	419	732	(C <sub>6</sub> H <sub>5</sub> )CH-CH=CH <sub>2</sub> , (C <sub>5</sub> H <sub>4</sub> N)CH=C=CH <sub>2</sub>
132	71	33	PVCH=CH <sub>2</sub> , HStCH=CH <sub>2</sub>
165	52	662	C <sub>13</sub> H <sub>10</sub> ,
194	225	746	[St <sub>2</sub> - CH <sub>2</sub> ]
207	377	872	[St <sub>2</sub> - H]
208	150	743	St <sub>2</sub> ; Dimer
210	161	52	VP <sub>2</sub> ; Dimer
211	42	23	VP <sub>2</sub> H
223	157	19	VP <sub>2</sub> (CH), St <sub>2</sub> CH <sub>3</sub>
267	3.1	93	C <sub>21</sub> H <sub>15</sub>
281	12	339	C <sub>22</sub> H <sub>17</sub>
298	7.6	69	[St <sub>3</sub> - CH <sub>2</sub> ], C <sub>23</sub> H <sub>21</sub>
306	6.1	484	C <sub>24</sub> H <sub>18</sub>
312	13.5	139	St <sub>3</sub> Trimer
315	2.5	3.4	VP <sub>3</sub> Trimer
316	4.8	1.6	VP <sub>3</sub> H
328	7.4	4.5	VP <sub>2</sub> (C <sub>6</sub> H <sub>5</sub> )CH-CH=CH <sub>2</sub>
355	2.6	82	C <sub>27</sub> H <sub>31</sub>
401	0.3	31	C <sub>31</sub> H <sub>29</sub> , [St <sub>4</sub> - CH]
416	0.8	6.7	St <sub>4</sub> Tetramer
429	1.1	35	St(C <sub>6</sub> H <sub>5</sub> )CH-CH=CH <sub>2</sub> , C <sub>33</sub> H <sub>33</sub>

In Figure 3-23 single ion evolution profiles (SIP) of some selected characteristic products are shown.

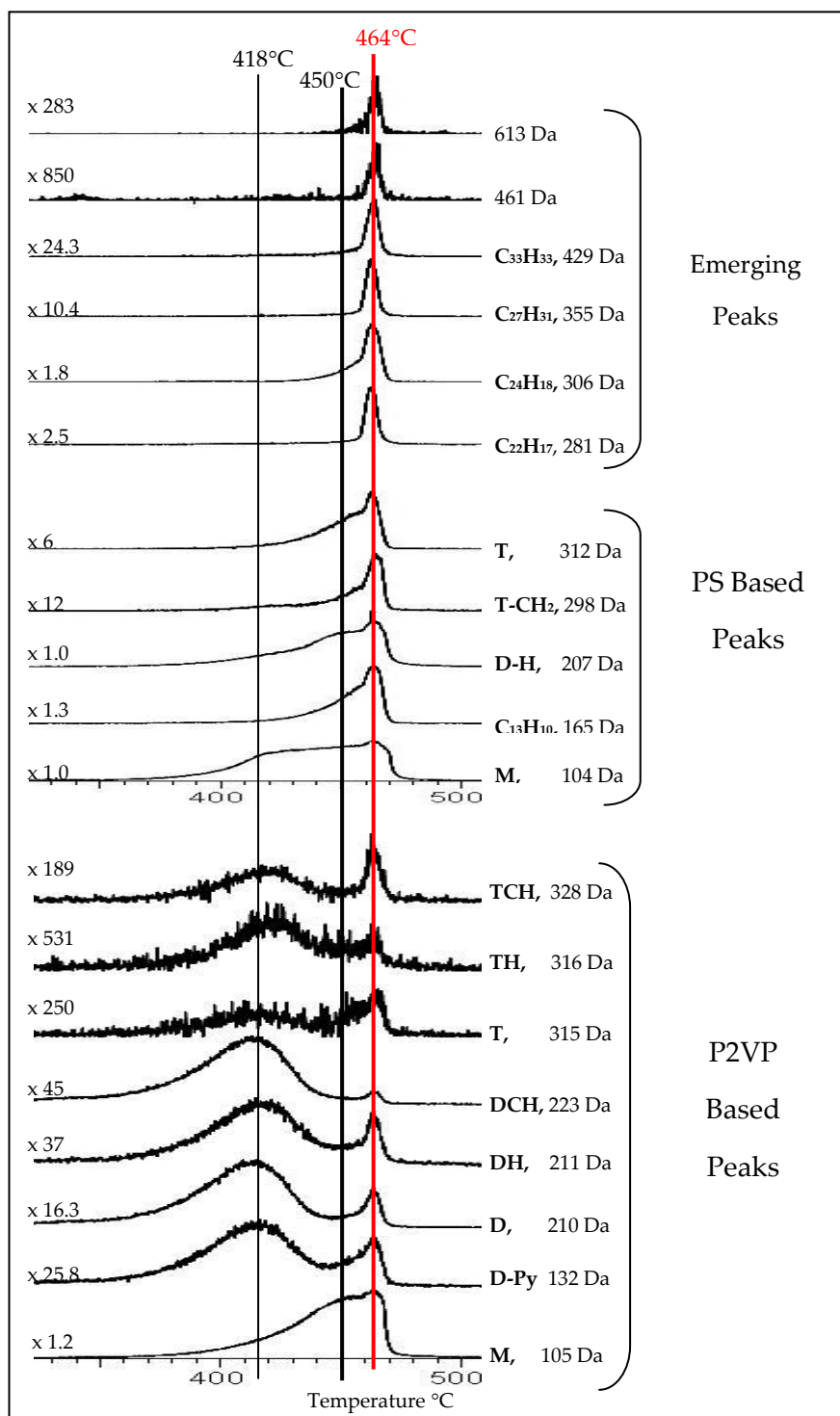


Figure 3-23: SIP of some selected characteristic products of Co-PS-b-P2VP polymer.

As can be seen in Figure 3-23, the trends observed in the evolution profiles and relative intensities of both P2VP and PS based products changed significantly, especially the relative intensities of P2VP based products diminished about 3-folds. The evolution profiles of P2VP based products were sharpened and shifted to higher temperatures. The relative intensities of the protonated oligomer peaks showed a decrease more than those of relative intensities of the oligomer peaks. Moreover, a high temperature peak appeared in the single ion evolution profiles of P2VP based products.

The changes in the evolution profiles and the relative intensities of the PS and P2VP based products are signs of new interactions that affect the thermal stability of the diblock copolymer. Diminish in the relative intensities of the protonated oligomer peaks of P2VP polymer can be attributed to a change in the thermal decomposition mechanism; the proton transfer reactions to the nitrogen atom were inhibited. Two distinct decomposition ranges were detected in the evolution profiles of products due to decomposition of P2VP block, one at 418 °C and the other at 464 °C. This is an indication of the presence of P2VP chains having different thermal stabilities. The presence of low temperature peak with a maximum at 418 °C, close to the value detected in the evolution profiles of P2VP based products during the pyrolysis of PS-*b*-P2VP diblock copolymer, is an indication of the existence of unreacted 2-vinylpyridine chains. On the other hand, the high temperature peak can directly be attributed to decomposition of chains involving cobalt metal atoms coordinated to nitrogen atom in the pyridine ring causing a significant increase in the thermal stability.

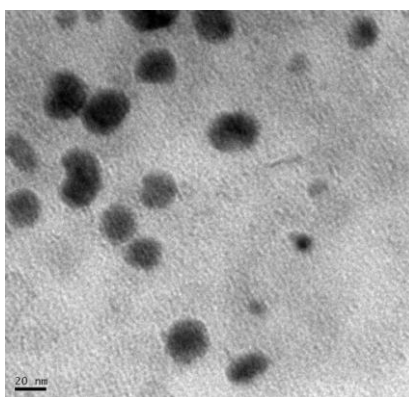
The emerged peaks due to the products with  $m/z$  values of 267, 281, 306, 325, 355, 429, 461, 613 Da were also inspected carefully. Their single ion pyrograms showed only a single and sharp peak with a maximum at 464 °C. Thus, it can be concluded that high temperature evolutions were mainly due to the

decomposition of the chains involving conjugated double bonds and/or crosslinked structures generated along the P2VP backbone upon cleavage of pyridine units coordinated to metal. After the loss of pyridine units coordinated to Co metal, the polymer backbone should have  $C_xH_y$  structure where  $x \geq y$  (Table 3-6). The decomposition of the chains should yield products with the same mass to charge ratio with products due to decomposition of PS chains and should make contributions to the intensities of related peaks in the mass spectrum.

Thus, it can be concluded that thermal degradation behavior of P2VP chains uncoordinated to Co metal, or PS chains far from the P2VP blocks coordinated to metal were similar to PS-*b*-P2VP diblock copolymer. On the other hand, thermal stability and thermal degradation mechanism of blocks involving Co atoms coordinated to N changed significantly as given in Scheme 3-3.

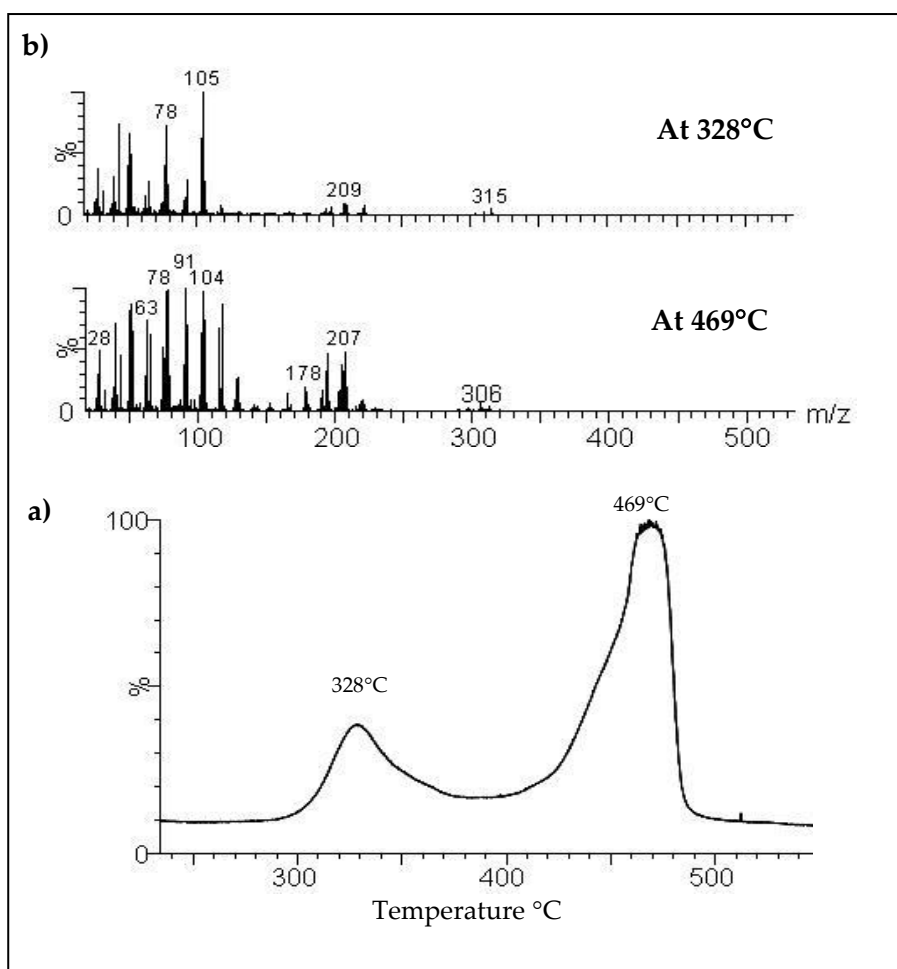
#### **3.2.4 Cobalt-PS-*b*-P4VP Diblock Copolymer**

Figure 3-24 shows cobalt particle distribution in PS-*b*-P4VP diblock copolymer matrix. Nano sized particle formation was achieved but it is clear from the image that cobalt metal coordination to P4VP was not as effective as it was in case of PS-*b*-P2VP.



**Figure 3-24:** TEM images of Co-PS-*b*-P4VP

The TIC curve and the pyrolysis mass spectra at the two peak maxima, at 469°C and at 328°C recorded during the pyrolysis of cobalt functional PS-b-P4VP are shown in Figure 3-25.



**Figure 3-25:** a) The TIC curve and b) Spectrum at the two peak maxima for Co-PS-b-P4VP

The thermal degradation temperature for the metal functional copolymer shifted almost 30 °C to 469 °C (Figure 3-26). Interestingly poly(4-vinylpyridine) degradation region remained almost unchanged. This is an indication of presence of numerous pyridine rings of P4VP uncoordinated to the cobalt metal. Still, the

evolution of some products that can be associated with thermal decomposition of chains involving pyridine units coordinated to metal, such as the one with  $m/z=306$  Da and the shift of the maximum of the second peak to higher temperatures are the evidences for the presence of metal functional P4VP chains.

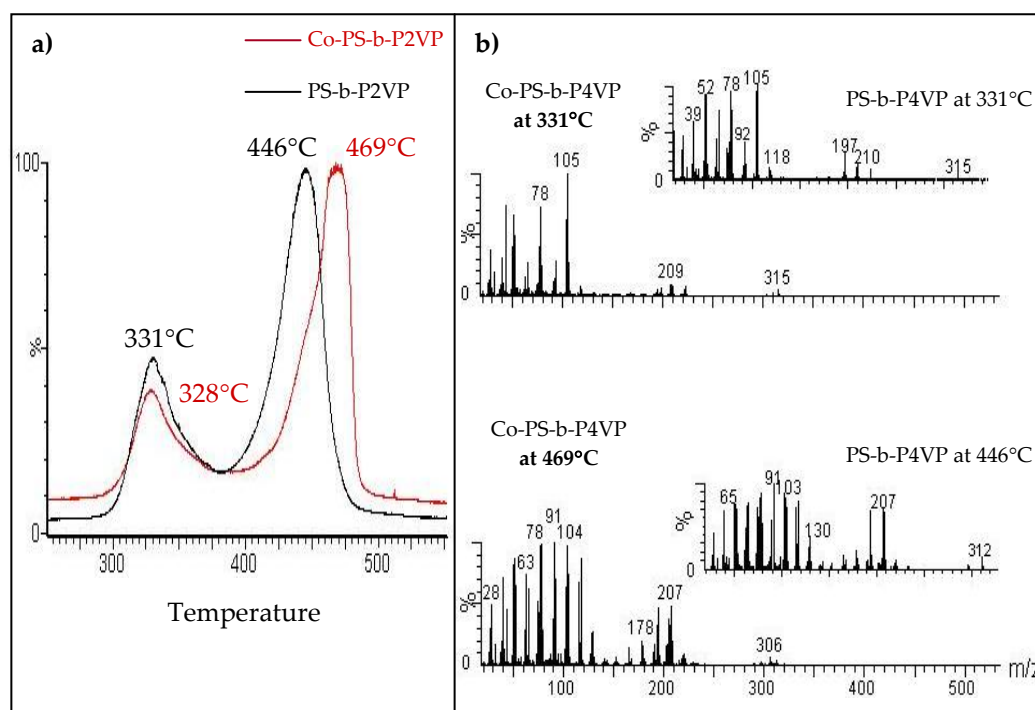


**Figure 3-26:** Comparison of the metal functional polymer with PS-b-P4VP a) TIC curves and b) Pyrolysis mass spectra

The relative intensities and the assignments made for the intense and/or characteristic peaks for the Co-PS-b-P4VP copolymer are collected in Table 3-7. Compared to PS-b-P2VP, the relative intensities of characteristic peaks at 267, 281, 306, 429, and 355 Da associated with decomposition of blocks coordinated to metal atom.

**Table 3-7:** Peak assignments for Co-PS-b-P4VP

m/z	RI at 328 °C	RI at 469 °C	ASSINGMENT
91	110	1000	C <sub>7</sub> H <sub>7</sub> , C <sub>6</sub> NH <sub>5</sub>
104	613	971	St, C <sub>8</sub> H <sub>8</sub> , [VP-H]
105	1000	733	StH, VP
106	271	68	VPH
117	70	866	(C <sub>6</sub> H <sub>5</sub> )CH-CH=CH <sub>2</sub> , (C <sub>5</sub> H <sub>4</sub> N)CH=C=CH <sub>2</sub>
132	21	11	PVCH=CH <sub>2</sub> , HStCH=CH <sub>2</sub>
165	9	5.2	C <sub>13</sub> H <sub>10</sub> ,
194	39	459	[St <sub>2</sub> - CH <sub>2</sub> ]
207	82	481	[St <sub>2</sub> - H]
208	19	195	St <sub>2</sub> ; Dimer
210	72	6.1	VP <sub>2</sub> ; Dimer
211	15	2.5	VP <sub>2</sub> H
223	30	2.6	VP <sub>2</sub> (CH), St <sub>2</sub> CH <sub>3</sub>
267	1	1	C <sub>21</sub> H <sub>15</sub>
281	3	3.5	C <sub>22</sub> H <sub>17</sub>
298	0.4	10.6	[St <sub>3</sub> - CH <sub>2</sub> ], C <sub>23</sub> H <sub>21</sub>
306	0.9	59	C <sub>24</sub> H <sub>18</sub>
312	0.8	39	St <sub>3</sub> Trimer
315	46	1.6	VP <sub>3</sub> Trimer
316	9	0.5	VP <sub>3</sub> H
328	0.8	0.4	VP <sub>2</sub> (C <sub>6</sub> H <sub>5</sub> )CH-CH=CH <sub>2</sub>
355	0.3	0.3	C <sub>27</sub> H <sub>31</sub>
401	0.2	3.6	C <sub>31</sub> H <sub>29</sub> , [St <sub>4</sub> - CH]
416	0.2	0.9	St <sub>4</sub> Tetramer
429	0	0.9	St <sub>3</sub> (C <sub>6</sub> H <sub>5</sub> )CH-CH=CH <sub>2</sub> , C <sub>33</sub> H <sub>33</sub>

In Figure 3-27 single ion evolution profiles of some selected characteristic products are shown.

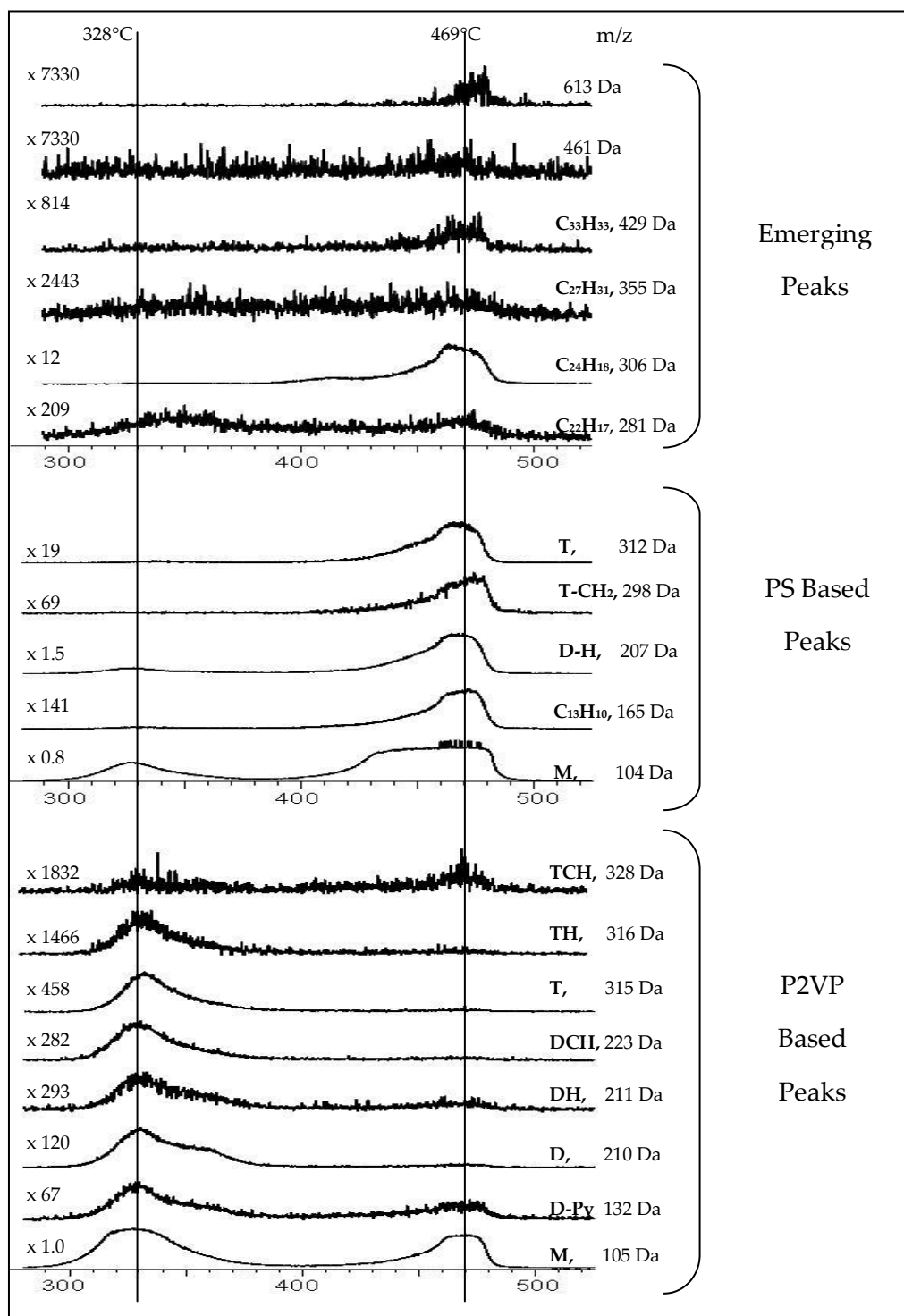


**Figure 3-27:** Single ion evolution profiles of some selected characteristic products of Co-PS-b-P4VP polymer

The relative intensities of P4VP based products are noticeably decreased as in case of Co-PS-b-P2VP (Figure 3-27). Yet, the decrease was less significant for this sample. Furthermore, the relative intensities of emerging peaks at 281, 355, and 461 Da were also quite low. Upon coordination of pyridine to metal, the high temperature peak in the evolution profiles of P2VP and PS shifted about 20 °C to high temperatures. This shift was 40 °C for the case of the Co-PS-b-P2VP. Thus, it can be concluded that extent of metal coordination for PS-b-P4VP was less than that was for PS-b-P2VP as also can be detected in the TEM image.

## CHAPTER 4

### CONCLUSION

Direct pyrolysis mass spectrometry studies indicated that;

- Both poly(2-vinylpyridine) and poly(4-vinylpyridine) homopolymers degrade by depolymerization reactions yielding mainly monomer and low molecular weight oligomers as in the case of most of the vinyl polymers. However, for P2VP, opposing reactions, proton transfer to N atom yielding unsaturated linkages on the polymer backbone which in turn increases thermal stability and loss of pyridine also take place. P4VP is thermally less stable than P2VP.
- During the thermal decomposition of diblock copolymers, PS-b-P2VP and PS-b-P4VP both components decomposed independently. Degradation occurs in two main steps, the thermally less stable P2VP or P4VP chains degrade in the first step and in the second step decomposition of PS takes place.
- TEM imaging confirmed generation of nanoparticles upon coordination of Co to P2VP or P4VP. Both TEM and pyrolysis mass spectrometry results indicated that PS-b-P2VP is a better matrix for metal bonding. The particle distribution is much better and more effective than PS-b-P4VP polymer.

- It was noted that upon coordination of metal, thermal stability of both P2VP and P4VP increased significantly. For metal functional PS-b-P2VP and PS-b-P4VP diblock polymers, again, uncoordinated vinyl chains and PS decomposed independently. Thermal degradation of chains coordinated to Co metal through N in the pyridine ring occurred in three steps; cleavage of pyridine coordinated to Co, coupling and H-transfer reactions yielding unsaturated and/or crosslinked structure and decomposition of these thermally more stable unsaturated and/or crosslinked blocks.

## REFERENCES

- [1] Williams, K. A., Boydston, A. J., Bielawski, C. W., *Chemical Society Reviews*, 36 ,(2007), Pages 729–744. (and references therein)
  
- [2] Baranauskas III, V. V., Zalich, M. A., Saunders, M., St. Pierre, T. G. and Riffle, J. S., *Chemical Materials*, 17, (2005), Page 5254.
  
- [3] Borrachero, M. V., Payá, J., Bonilla, M., Monzo, J.; *Journal of Thermal Analysis and Calorimetry*, 91, (2008), 2, Pages 503–509
  
- [4] Hacaloglu, J., “Pyrolysis Mass Spectrometry For Molecular Ionization Methods”, *The Encyclopedia Of Mass Spectrometry: Ionization Methods*, Vol. 6, Edited by Gross, M. L., et al., Elsevier Science Ltd, (2007), Pages 925-938
  
- [5] Georgakopoulos, C. G., Statheropoulos, M. C., Montaudo, G., *Polymer Degradation and Stability*, 61, Issue 3, (1998), Pages 481-491
  
- [6] Georgakopoulos, C. G., Statheropoulos, M. C., Montaudo, G., *Analytica Chimica Acta*, 359, Issues 1-2, 19 , (February 1998), Pages 213-225
  
- [7] Qian, K., Killinger, W. E., Casey, M. Nicol, G. R.; *Analytical Chemistry*, (1996), 68, Pages 1019-1027 (and references therein)
  
- [8] 09 February 2008, Van Bramer S. E., An Introduction to Mass Spectrometry, <http://science.widener.edu/svb/massspec/masspec.html>, (1998)

- [9] 09 February 2008, Ashcroft, A. E., "An Introduction to Mass Spectrometry", <http://www.astbury.leeds.ac.uk/facil/MStut/mstutorial.html>
- [10] Gross, J. H., *Mass Spectrometry a Textbook*, Springer-Verlag Berlin Heidelberg, (2004), (and references therein)
- [11] 05 July 2008, MDS Sciex, <http://www.mdsciex.com/products/about%20mass%20spectrometry/#work>
- [12] Montaudo, G., Lattimer R. P., *Mass Spectrometry of Polymers*, CRC Press; 1<sup>st</sup> edition, (2001), Page 3, 19
- [13] 09 February 2008, Princeton University, <http://www.princeton.edu/~polymer/block.html>
- [14] 09 February 2008, Pine, J. D., "Nanoparticles in Copolymers", <http://www.physics.nyu.edu/pine/research/nanocopoly.html>, (March 2007)
- [15] Li, M., Ober C. K., *Materials Today*, 9, (September 2006), Number 9, Pages 30-39 (and references therein).
- [16] Park, C., Yoon, J., Thomas E. L., *Polymer*, 44, (2003), Pages 6725–6760
- [17] Chen, Z., Kornfield, J. A., Smith, S. D., Grothaus, J. T., Satkowski, M. M., *Science*, 277, (1997), Pages 1248-1253 (and references therein).
- [18] Hadjichristidis, N., Pitsikalis, M., Iatrou, H., *Advances in Polymer Science*, 189, (2005), Pages 1–124
- [19] Lodge, T. P., *Macromolecular Chemistry and Physics*, 204, (2003), Pages 265–273

- [20] 09 February 2008, "Synthesis of Poly(styrene-b-2-vinylpyridine) by Living Anionic Polymerization" , <http://english.che.ncku.edu.tw/papers/B-Functional/B070.pdf>
- [21] Ramos, J., Millan, A., Palacio, F., *Polymer*, 41, (2000), Pages 8461–8464
- [22] Kim, B. J., Chiu, J. J., Yi, G. R., Pine, D. J. and Kramer., E. J., *Advanced Materials*, 17, (2005), Pages 2618-2622
- [23] Grubbs, R. B., *Journal of Polymer Science*, 43, (2005), Page 4323
- [24] Lo, C. T., Lee, B., Dietz-Rago, N. L., Winans, R. E., Thiyagarajan, P., *Macromolecular Rapid Communications*, 28, (2007), Pages 1607-1612.
- [25] Chiu, J. J., Kim, B. J., Kramer, E. J. *Journal of the American Chemical Society*, 127, (2005), Pages 5036-5037
- [26] Chai, J., Wang, D., Fan, X., Buriak, J. M., *Nature Nanotechnology*, 2, (August 2007), Pages 500-506
- [27] Ohtani, H., Yuyama, T., Tsuge, S., Plage, B., Schulten, H. R., *European Polymer Journal*, 26, (1990), Pages 893-899
- [28] Shibasaki, Y. and Yang, M., *Journal of Thermal Analysis*, 49, (1997), Page 71
- [29] Luderwald, I. and Vogl, O., *Macromolecular Chemistry*, 180, (1972), Page 2302.
- [30] Guaita, M., *British Polymer Journal*, 18, (1986), Page 226
- [31] Shapi, M. M., Hesso, A., *Journal of Analytical and Applied Pyrolysis*, 18, (1990), Page 143

- [32] Ohtani, H., Ueda, S., Tsukahama, Y., Watanabe, C. and Tsuge, S., *Journal of Analytical and Applied Pyrolysis*, 25, (1993), Pages 1-10
- [33] Faravelli, T., Pinciroli, M., Pisano, F., Bozzano G., Dente, M., Ranzi, E., *Journal of Analytical and Applied Pyrolysis*, 60, (2001), Pages 103–121
- [34] Kroschwitz, J. I., *Concise Encyclopedia of Polymer Science and Engineering*, John Wiley & Sons, NY, (1990), Pages 1284-1285
- [35] Sivudu, K. S., Shailaja, D., *Journal of Applied Polymer Science*, 100, Issue 5, (2006), Pages 3439-3445
- [36] Grzyb, B., Machnikowski, J., Weber J. V., *Journal of Analytical and Applied Pyrolysis*, 72, (2004), Pages 121–130
- [37] Kuo, S. W., Lin, C. L., Chang, F. C., *Polymer*, 43, (2002), Pages 3943-3949
- [38] Zha, W., Han, C. D., Lee, D. H., Han, S. H., Kim, J. K., Kang, J. H., Park, J., *Macromolecules*, 40, (2007), Pages 2109-2119
- [39] Zalich, M. A., Saunders, M., Baranauskas, V. V., Vadala, M. L., Riffle, J. S. and St. Pierre T. G., *Microscopy and Microanalysis*, 11 (Suppl. 2), (2005), Pages 1898-1899
- [40] M. de Silva, R., Palshin, V., Fronczek, F. R., Hormes, J. and Kumar, C. S. S. R., *Journal of Physical Chemistry C*, 111, (2007), Pages 10320-10328
- [41] Kaleli, K., "Nano Structural Metal Composites: Synthesis, Structural and Thermal Characterization", *Master of Science Thesis*, Middle East Technical University, Graduate School of Natural and Applied Science, Department of Chemistry, 2008